J|A|C|S
ARTICLES
Published on Web 04/02/2002

Cooperative Self-Assembly of Dendrimers via Pseudorotaxane Formation from a Homotritopic Guest Molecule and Complementary Monotopic Host Dendrons

Harry W. Gibson,* Nori Yamaguchi, Lesley Hamilton, and Jason W. Jones

Contribution from the Department of Chemistry, Virginia Polytechnic Institute & State University, Blacksburg, Virginia 24061

Received September 10, 2001. Revised Manuscript Received October 8, 2001

Abstract: Interaction of the homotritopic guest 1,3,5-tris[*p*-(benzylammoniomethyl)phenyl]benzene tris(hexafluorophosphate) (**1a**) with dibenzo-24-crown-8 (DB24C8) leads to the sequential self-assembly of [2]-, [3]-, and [4]-pseudorotaxanes **7a**, **8a**, and **9a**, respectively. The self-assembly processes were studied using NMR spectroscopy. In CD_3CN and CD_3COCD_3 the individual association constants K_1, K_2, and K_3 for 1:1, 1:2, and 1:3 complexes were determined by several methods. Via Scatchard plots, the three NH_2^+ sites of **1a** were shown to behave independently in binding DB24C8. K values (4.4×10^2, 1.4×10^2, and 41 M^{-1}, respectively, in CD_3CN) directly determined from signals for the individual complexes (**7a**, **8a**, and **9a**) were somewhat higher than those estimated from the Scatchard plot because of concentration dependence, but the ratios of association constants followed the expected statistical order ($K_1:K_2:K_3 = 3:1:{}^1/_3$). These are believed to be the first evaluations of association constants leading to a [4]-pseudorotaxane. In the less polar $CDCl_3$, association constants could not be determined because ~90% of the dissolved tritopic guest, which by itself is insoluble, was present as the fully loaded [4]pseudorotaxane **9a**! Self-assembly of homotritopic guest **1a** with benzyl ether dendrons of the first, second, and third generations functionalized at the "focal point" with DB24C8 moieties (**3**−**5**) produces pseudorotaxane dendrimers. The self-assembly processes were studied using ^1H NMR spectroscopy. In CD_3COCD_3 for all three generations the individual association constants K_1, K_2, and K_3 for [2]-, [3]-, and [4]-pseudorotaxane complexes **7c**−**e**, **8c**−**e**, and **9c**−**e** indicated that *the self-assembly was cooperative*; that is, the ratios of the individual association constants exceeded the expected statistical ratios. Scatchard plots confirmed this behavior. Self-assembly processes in the less polar $CDCl_3$ were kinetically slow, requiring ca. 1, 2, and 3 days, respectively, for the first, second, and third generation systems to reach equilibrium with **1a**; the slow rate is attributed to the insolubility of the homotritopic guest **1a** in this medium and the steric demands of the resulting dendrimers. However, *only dendrimers of 1:3 stoichiometry, that is, the nanoscopic [4]-pseudorotaxanes **9**, were formed!* Moreover, it is noteworthy that the extent of dissolution of **1a** (reflective of the overall association constant which is too high to measure) increases with generation number, presumably because of the more effective screening of the ionic guest by the larger dendrons and perhaps favorable $\pi-\pi$ and CH$-\pi$ interactions. Such cooperative effects suggest a number of applications that can take advantage of the pH-switchable nature of these self-assembly processes.

Introduction

Supramolecular chemistry has developed rapidly as scientists around the world endeavor to produce nanoscopically controlled multicomponent structures with designed functionality.[1] Pseudorotaxanes and rotaxanes,[2] mechanically linked molecular compounds in which a cyclic molecule is threaded by a linear molecule, are an important subset of such self-assembled structures.

Dendrimers with their large and controllable numbers of end groups, unique shapes, and physical properties provide an almost endless array of possibilities for design of materials with targeted end-use functionalities.[3] Thus, dendrimers are beginning to find potential applications in the fields of photo- and electroactive materials,[4] bioactive agents,[5] catalysis,[6] encapsulation and delivery,[7] sensors/diagnostics,[8] and membrane chemistry.[9] However, structural control and synthetic efficiency still remain major issues in dendrimer research.[10] Three methods (convergent,[11] divergent,[12] and double-stage convergent[13]) are recognized for high molecular weight, monodisperse dendrimer synthesis.

* To whom correspondence should be addressed. E-mail: hwgibson@vt.edu.

(1) Vögtle, F. *Supramolecular Chemistry*; John Wiley and Sons: New York, 1991. Cram, D. J.; Cram, J. M. *Container Molecules and Their Guests*; Royal Society of Chemistry: Cambridge, U.K., 1994. Lehn, J.-M. *Supramolecular Chemistry*; VCH Publishers: New York, 1995. *Comprehensive Supramolecular Chemistry*; Atwood, J. L., Davies, J. E. D., MacNicol, D. D., Vögtle, F., Eds.; Pergamon Press: New York, 1996. Moore, J. S. *Curr. Opin. Colloid Interface Sci.* **1999**, *4*, 108−116. Caulder, D. L.; Raymond, K. N. *Acc. Chem. Res.* **1999**, *32*, 975−982. Rowan, A. E.; Elemans, J. A. A. W.; Nolte, R. J. M. *Acc. Chem. Res.* **1999**, *32*, 995−1006. Leininger, S.; Olenyuk, B.; Stang, P. J. *Chem. Rev.* **2000**, *100*, 853−908. *Self-Assembly in Supramolecular Systems*; Lindoy, L. F., Atkinson, I. M., Eds.; Royal Society of Chemistry: Cambridge, U.K., 2000. Ozin, G. A. *Chem. Comun.* **2000**, 419−432. Steed, J. W.; Atwood, J. L. *Supramolecular Chemistry*; Wiley and Sons: New York, 2000. Holliday, B. J.; Mirkin, C. A. *Angew. Chem., Int. Ed.* **2001**, *40*, 2022−2043. Brunsveld, L.; Folmer, B. J. B.; Meijer, E. W.; Sijbesma, R. P. *Chem. Rev.* **2001**, *101*, 4071−4098.

Zimmerman et al. introduced a self-assembly approach, which guarantees structural accuracy, while eliminating steps from the conventional multistep covalent approach.[14] In this case, six subunits were brought together by hydrogen bonding to construct supramolecular dendritic structures up to the fourth generation. Percec et al. achieved supramolecular dendrimers based on building block shape and size and the interactions of the focal point moieties.[15] Recently, supramolecular chemistry has been used to attach other functionalities to the surfaces of dendrimers in a noncovalent manner.[16]

Our ultimate aim is to devise methods utilizing multitopic guest/host systems to prepare precisely controlled multilayered dendritic assemblies by use of orthogonal guest/host pairs.

Scheme 1. Cartoon Representations of Formation of [2]-, [3]-, and [4]-Pseudorotaxane Complexes **7**, **8**, and **9** from Homotritopic Guest **1a** and DB24C8 and Derivatives **2b**, **3**−**5**[a]

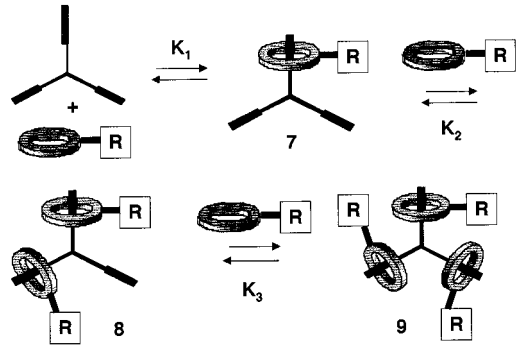

[a] a, R = H, b, R = $COOCH_3$, c, R = $COOCH_2G1$, d, R = $COOCH_2G2$, e, R = $COOCH_2G3$.

Because of the selectivity of the host imbued by the size and shape of the cavity, pseudorotaxanes are ideally suited for the construction of such nano-objects. In nature, this sort of process is exemplified by viruses, which can form rodlike, filamentous, helical, or polydedral aggregates consisting of proteins self-assembled about a nucleic acid.[17]

As a beginning toward this goal, we have examined using ^{1}H NMR spectroscopy self-assembly of a tritopic guest species, first with a simple host, and then with dendron-functionalized hosts to form pseudorotaxanes as described in a preliminary account.[18] In this paper, we describe equilibrium studies of these [2]-, [3]-, and [4]-pseudorotaxane complexes, culminating in what we believe are the first self-assembled pseudorotaxane dendrimers.

Results and Discussion

Our strategy for self-assembling [4]pseudorotaxane dendrimers is illustrated in Scheme 1. A homotritopic building block for the core was designed to have three arms, each containing a guest moiety (represented by the filled rectangle) capable of binding the host moieties, represented by circles or ellipses, located at the focal points of first, second, and third generation dendrons. Stoddart et al. reported that dibenzo-24-crown-8 (DB24C8) and other crown ethers form pseudorotaxanes with secondary ammonium salts.[19] Association constants were estimated by ^{1}H NMR for the [2]pseudorotaxanes and a single [3]-

(2) For reviews of pseudorotaxanes and rotaxanes, see: (a) Amabilino, D. B.; Stoddart, J. F. *Chem. Rev.* **1995**, *95*, 2725−2828. (b) Gibson, H. W. In *Large Ring Molecules*; Semlyen, J. A., Ed.; John Wiley and Sons: New York, 1996; Chapter 6, pp 191−262. (c) Nepolgodiev, S. A.; Stoddart, J. F. *Chem. Rev.* **1998**, *98*, 1959−1976. (d) Raymo, F. M.; Stoddart, J. F. *Chem. Rev.* **1999**, *99*, 9, 1643−1664. (e) Fyfe, M. C. T.; Stoddart, J. F. *Adv. Supramol. Chem.* **1999**, *5*, 1−53. (f) *Molecular Catenanes, Rotaxanes, and Knots*; Sauvage, J.-P., Dietrich-Buchecker, C. O., Eds.; Wiley-VCH: Weinheim, 1999. (g) Dietrich-Buchecker, C.; Rapenne, G.; Sauvage, J.-P. Chapter 6 in ref 2f, pp 107−142. (h) Heim, C.; Udelhofen, D.; Vögtle, F. Chapter 8 in ref 2f, pp 177−222. (i) Gong, C.; Gibson, H. W. Chapter 11 in ref 2f, pp 277−321. (j) Hubin, T. J.; Busch, D. H. *Coord. Chem. Rev.* **2000**, *200*−*202*, 5−52. (k) Cantrill, S. J.; Pease, A. R.; Stoddart, J. F. *J. Chem. Soc., Dalton Trans.* **2000**, 3715−3734. (l) Mahan, E.; Gibson, H. W. In *Cyclic Polymers*, 2nd ed.; Semlyen, J. A., Ed.; Kluwer Publishers: Dordrecht, 2000; pp 415−560.

(3) Newkome, G. R.; Moorefield, C. N.; Vögtle, F. *Dendritic Molecules: Concepts, Synthesis, Perspectives*; VCH: Weinheim, 1996. Matthews, O. A.; Shipway, A. N.; Stoddart, J. F. *Prog. Polym. Sci.* **1998**, *23*, 1−56. Bosman, A. W.; Janssen, H. M.; Meijer, E. W. *Chem. Rev.* **1999**, *99*, 1665−1688. Newkome, G. R.; He, E.; Moorefield, C. N. *Chem. Rev.* **1999**, *99*, 1689−1746. Tully, D. C.; Fréchet, J. M. J. *Chem. Commun.* **2001**, 1229−1239. Grayson, S. M.; Fréchet, J. M. J. *Chem. Rev.* **2001**, *101*, 3819−3868.

(4) Freeman, A. W.; Koene, C.; Malenfant, P. R. L.; Thompson, M. E.; Fréchet, J. M. J. *J. Am. Chem. Soc.* **2000**, *122*, 12385−12386. Weener, J.-W.; Meijer, E. W. *Adv. Mater.* **2000**, *12*, 741−746. Schenning, A. P. H. J.; Peeters, E.; Meijer, E. W. *J. Am. Chem. Soc.* **2000**, *122*, 4489−4495. Baars, M. W. P. L.; van Boxtel, M. C. W.; Bastiaansen, C. W. M.; Broer, D. J.; Sontjens, S. H. M.; Meijer, E. W. *Adv. Mater.* **2000**, *12*, 715−719. Malenfant, P. R. L.; Fréchet, J. M. J. *Macromolecules* **2000**, *33*, 3634−3640. Newkome, G. R.; Narayanan, V. V.; Godinez, L. A. *J. Org. Chem.* **2000**, *65*, 1643−1649. Newkome, G. R.; He, E.; Godínez, L. A.; Baker, G. R. *J. Am. Chem. Soc.* **2000**, *122*, 9993−10006. Lupton, J. M.; Samuel, I. D. W.; Beavington, R.; Burn, P. L.; Bässler, H. *Adv. Mater.* **2001**, *13*, 258−261. Maus, M.; De, R.; Lor, M.; Weil, T.; Mitra, S.; Wiesler, U.-M.; Herrmann, A.; Hofkens, J.; Vosch, T.; Müllen, K.; De Schryver, F. C. *J. Am. Chem. Soc.* **2001**, *123*, 7668−7676. Toba, R.; Quintela, J. M.; Peinador, C.; Roman, E.; Kaifer, A. E. *Chem. Commun.* **2001**, 857−858.

(5) Choi, J. S.; Lee, E. J.; Choi, Y. H.; Jeong, Y. J.; Park, J. S. *Bioconjugate Chem.* **1999**, *10*, 62−65. Choi, J. S.; Joo, D. K.; Kim, C. H.; Kim, K.; Park, J. S. *J. Am. Chem. Soc.* **2000**, *122*, 474−480. Balogh, L.; Swanson, D. R.; Tomalia, D. A.; Hagnauer, G. L.; McManus, A. T. *Nano Lett.* **2001**, *1*, 18−21. Kobayashi, H.; Kawamoto, S.; Saga, T.; Sato, N.; Ishimori, T.; Konishi, J.; Ono, K.; Togashi, K.; Brechbiel, M. W. *Bioconjugate Chem.* **2001**, *12*, 587−593.

(6) Oosterom, G. E.; Reek, J. N. H.; Kamer, P. C. J.; van Leeuwen P. W. N. M. *Angew. Chem., Int. Ed.* **2001**, *40*, 1828−1849. Zhou, M.; Roovers, J. *Macromolecules* **2001**, *34*, 244−252. Hecht, S.; Fréchet, J. M. J. *J. Am. Chem. Soc.* **2001**, *123*, 6959−6960. Niu, Y.; Yeung, L. K.; Crooks, R. M. *J. Am. Chem. Soc.* **2001**, *123*, 6840−6846. Astruc, D.; Chardac, F. *Chem. Rev.* **2001**, *101*, 2991−3024.

(7) Baars, M. W. P. L.; Kleppinger, R.; Koch, M. H. J.; Yeu, S.-L.; Meijer, E. W. *Angew. Chem., Int. Ed.* **2000**, *39*, 1285−1288. Gorman, C. B.; Smith, J. C. *Acc. Chem. Res.* **2000**, *34*, 60−71. Hecht, S.; Vladimirov, N.; Fréchet, J. M. J. *J. Am. Chem. Soc.* **2001**, *123*, 18−25. Marsitzky, D.; Vestberg, R.; Blainey, P.; Tang, B. T.; Hawker, C. J.; Carter, K. R. *J. Am. Chem. Soc.* **2001**, *123*, 6965−6972.

(8) Le Derf, F.; Levillain, E.; Trippe', G.; Gorgues, A.; Salle', M.; Sebastian, R.-M.; Caminade, A.-M.; Majoral, J.-P. *Angew. Chem., Int. Ed.* **2001**, *40*, 224−227. Gong, L.-Z.; Hu, Q.-S.; Pu, L. *J. Org. Chem.* **2001**, *66*, 2358−2367.

(9) Jansen, J. F. G. A.; de Brabander-van den Berg, E. M. M.; Meijer, E. W. *Science* **1994**, *266*, 1226−1229. Jansen, J. F. G. A.; Meijer, E. W. *J. Am. Chem. Soc.* **1995**, *117*, 4417−4418. Kovvali, A. S.; Sirkar, K. K. *Ind. Eng. Chem. Res.* **2001**, *40*, 2502−2511.

(10) Moore, J. S. *Acc. Chem. Res.* **1997**, *30*, 402−413.

(11) Wooley, K. L.; Hawker, C. J.; Fréchet, J. M. J. *J. Am. Chem. Soc.* **1991**, *113*, 4252−4261.

(12) Newkome, G. R.; Yao, Z.; Baker, G. R.; Gupta, V. K.; Russo, P. S.; Sanders, M. J. *J. Am. Chem. Soc.* **1986**, *108*, 849−850. Tomalia, D. A.; Baker, H.; Dewald, J.; Hall, M.; Kallos, G.; Martin, S.; Roeck, J.; Ryder, J.; Smith, P. *Macromolecules* **1986**, *19*, 2466−2468.

(13) Kawaguchi, T.; Walker, K. L.; Wilkins, C. L.; Moore, J. S. *J. Am. Chem. Soc.* **1995**, *117*, 2159−2165.

(14) Zimmerman, S. C.; Zeng, F.; Reichert, D. E. C.; Kolotuchin, S. V. *Science* **1996**, *271*, 1095−1098. Zeng, F.; Zimmerman, S. C. *Chem. Rev.* **1997**, *97*, 1681−1712.

(15) Percec, V.; Cho, W.-D.; Ungar, G.; Yeardley, D. J. P. *J. Am. Chem. Soc.* **2001**, *123*, 1302−1315.

(16) Nagaskai, T.; Kimura, O.; Masakatsu, U.; Arimori, S.; Hamachi, I.; Shinkai, S. *J. Chem. Soc., Perkin Trans. 1* **1994**, 75−81. Castro, R.; Cuadrado, I.; Alonso, B.; Casado, C. M.; Mora, M.; Kaifer, A. E. *J. Am. Chem. Soc.* **1997**, *119*, 5760−5761. Gonzalez, B.; Casado, C. M.; Alonso, B.; Cuadrado, I.; Moran, M.; Wang, Y.; Kaifer, A. E. *J. Chem. Soc., Chem. Commun.* **1998**, 2569−2570. Baars, M. W. P. L.; Karlsson, A. J.; Sorokin, V.; de Waal, B. F. W.; Meijer, E. W. *Angew. Chem., Int. Ed.* **2000**, *39*, 4262−4265. Boas, U.; Karlsson, A. J.; de Waal, B. F. M.; Meijer, E. W. *J. Org. Chem.* **2001**, *66*, 2136−2145. Michels, J. J.; Baars, M. W. P. L.; Meijer, E. W.; Huskens, J.; Reinhoudt, D. N. *J. Chem. Soc., Perkin Trans. 2* **2000**, 1914−1918. Lee, J. W.; Ko, Y. H.; Park, S.-H.; Yamaguchi, K.; Kim, K. *Angew. Chem., Int. Ed.* **2001**, *40*, 746−749. de Groot, D.; de Waal, B. F. M.; Reek, J. N. H.; Schenning, A. P. H. J.; Kamer, P. C. J.; Meijer, E. W.; van Leeuwen, P. W. N. M. *J. Am. Chem. Soc.* **2001**, *123*, 8453−8458. Gibson, H. W.; Bosman, A. W.; Bryant, W. S.; Jones, J. W.; Jannsen, R. A. J.; Meijer, E. W. *Polym. Mater. Sci. Eng.* **2001**, *84*, 66−67.

(17) Zubay, G. L. *Biochemistry*, 4th ed.; W. C. Brown Publishers: Boston, 1998; pp 101−106, 734−737.

(18) Yamaguchi, N.; Hamilton, L. M.; Gibson, H. W. *Angew. Chem., Int. Ed.* **1998**, *37*, 3275−3279.

Scheme 2. Structures and Proton Designations of Derivatized Dibenzo-24-crown-8 Compounds

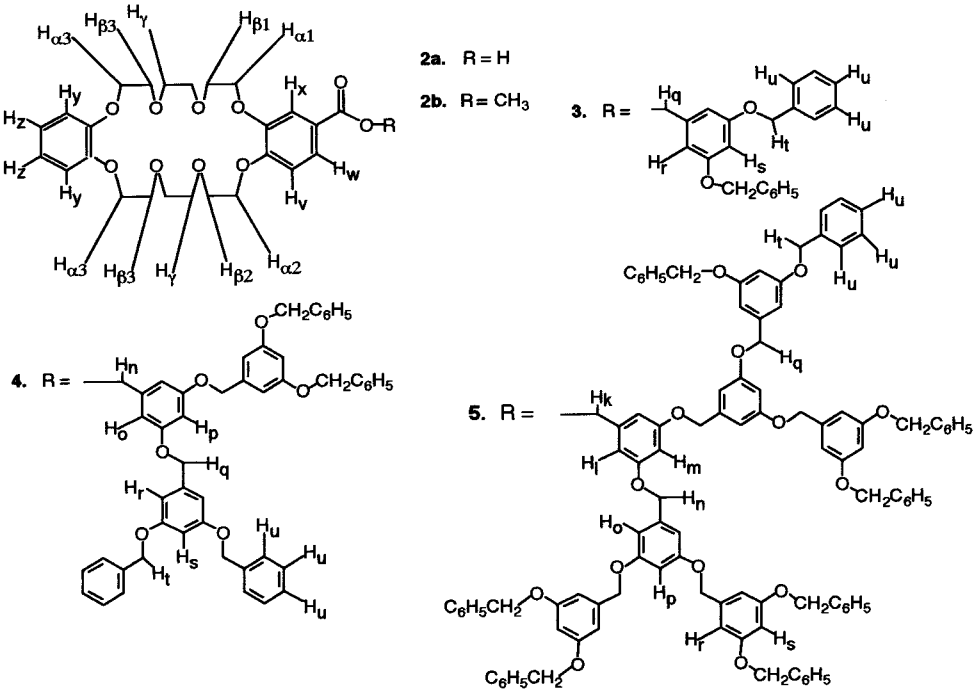

pseudorotaxane,[19e] but not for the very interesting [4]-, [5]-, and [6]-pseudorotaxanes.[19b,d,g] We chose to use this molecular recognition motif in our pursuit of dendritic pseudorotaxanes.

I. Building Blocks For Self-Assembly. 1,3,5-Tris(*p*-benzylammoniomethylphenyl)benzene tri(hexafluorophosphate) (**1a**)[18,20] exhibited good solubility in acetone and acetonitrile but not in chloroform and methylene chloride.

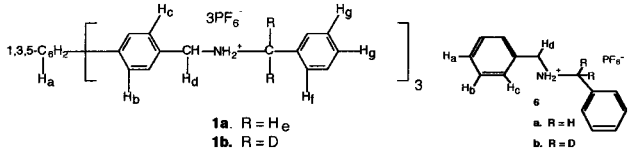

The benzylic alcohol moieties of the first three generations of benzyl ether dendrons[11] were coupled to 2-carboxydibenzo-24-crown-8 (**2a**), leading to the monotopic host dendrons **3**−**5** (Scheme 2).[18] Model ester **2b** was also prepared.[18] Molecular mechanics calculations on the targeted [4]pseudorotaxane dendrimers **9c**, **9d**, and **9e** (Scheme 1) yielded disk-shaped structures with approximate "diameters" of 8, 10, and 12 nm.

II. Model Complexation Studies. A. In CD_3CN. The ^1H NMR spectra in acetonitrile-d_3 were the most clearly resolved and provide a useful basis for discussion of the complexation processes in acetone and chloroform. As reported for **6a**/DB24C8,[19] sets of signals are observed for free and complexed DB24C8 and free and complexed ammonium salt moieties, due to slow association and dissociation relative to the ^1H NMR time scale.

As illustrated (Scheme 3a), when DB24C8 is complexed with the ammonium salt moiety of **1a**, there are at least six and as many as 12 nonequivalent sets of ethyleneoxy protons.[21] The signals for the uncomplexed benzylic protons, H_{du} and H_{eu}, of guest **1a** appear at 4.25 and 4.23 ppm, respectively, and move upfield as the crown ether concentration increases (see below for a discussion of possible reasons for this shift). The merged signal for these protons, H_{dc} and H_{ec}, in the [2]-, [3]-, and [4]-pseudorotaxane complexes **7a**, **8a**, and **9a** in turn (Scheme 4), is constant at 4.74 ppm.[21] The percentage of ammonium species complexed was determined by integration of these two sets of signals; it ranged from 26.5 to 95.8% at $[DB24C8]_o$ = 10 to 50 mM. In the presence of DB24C8, the signals for H_{du} and H_{eu} are more complicated than those of **1a** alone. This can be understood by reference to the structure of expected [2]pseudorotaxane **7a** (Scheme 4); note that the uncomplexed NCH_2 protons H_{du1} and H_{eu1} of the two arms exist as two diastereotopic pairs due to the asymmetry brought about by complex formation. However, in [3]pseudorotaxane **8a**, H_{du2} and H_{eu2} are equivalent within each pair. Yet in **8a**, H_{dc} and H_{ec} of the complexed arms each consist of diastereotopic pairs, as reflected in the additional fine structure observed in the 4.74 ppm signal.[21]

The aromatic protons of DB24C8 (Figure 1) can also be used to estimate the extent of complexation. The signal (6.80 ppm) for the complexed species (H_{Arc}) is shifted upfield, and the splitting pattern is simpler than that (6.92 ppm) of the uncom-

(19) (a) Ashton, P. R.; Campbell, P. J.; Chrystal, E. J. T.; Glink, P. T.; Menzer, S.; Philp, D.; Spencer, N.; Stoddart, J. F.; Tasker, P. A.; Williams, D. J. *Angew. Chem., Int. Ed. Engl.* **1995**, *34*, 1865−1869. (b) Ashton, P. R.; Chrystal, E. J. T.; Glink, P. T.; Menzer, S.; Schiavo, C.; Spencer, N.; Stoddart, J. F.; Tasker, P. A.; White, A. J. P.; Williams, D. J. *Chem.-Eur. J.* **1996**, *2*, 709−728. (c) Ashton, P. R.; Fyfe, M. C. T.; Hickingbottom, S. K.; Stoddart, J. F.; White, A. J. P.; Williams, D. J. *J. Chem. Soc., Perkin Trans. 2* **1998**, 2117−2128. (d) Fyfe, M. C. T.; Stoddart, J. F. *Adv. Supramol. Chem.* **1999**, *5*, 1−53. (e) Chang, T.; Heiss, A. M.; Cantrill, S. J.; Fyfe, M. C. T.; Pease, A. R.; Rowan, S. J.; Stoddart, J. F.; Williams, D. *Org. Lett.* **2000**, *2*, 2943−2946. (f) See: Rowan, S. J.; Cantrill, S. J.; Stoddart, J. F.; White, A. J. P.; Williams, D. J. *Org. Lett.* **2000**, *2*, 759−762 for complexation of **6a** with 2-formyldibenzo-24-crown-8 with reduced (but unmeasured) K_a relative to the unsubstituted crown. (g) Cantrill, S. J.; Pease, A. R.; Stoddart, J. F. *J. Chem Soc., Dalton Trans.* **2000**, 3715−3734. (h) Chang, T.; Heiss, A. M.; Cantrill, S. J.; Fyfe, M. C. T.; Pease, A. R.; Rowan, S. J.; Stoddart, J. F.; White, A. J. P.; Williams, D. J. *Org. Lett.* **2000**, *2*, 2947−2950. (i) Amirsakis, D. G.; Garcia-Garibay, M. A.; Rowan, S. J.; Stoddart, J. F.; White, A. J. P.; Williams, D. J. *Angew. Chem., Int. Ed.* **2001**, *40*, 4256−4261.

(20) Ashton, P. R.; Collins, A. N.; Fyfe, M. C. T.; Glink, P. T.; Menzer, S.; Stoddart, J. F.; Williams, D. J. *Angew. Chem., Int. Ed. Engl.* **1997**, *36*, 59−62.

(21) See Supporting Information.

Scheme 3. (a. Left) Representation of the Complexation Site between the Ammonium Salt Moiety of Homotritopic Guest **1a** and DB24C8, Designating the Diastereotopic Ethyleneoxy Protons Resulting from the Fact that the Two Faces of the Crown Ether Are Diastereotopic[a] and (b. Right) Representation of the Complexation Site between the Ammonium Salt Moiety of Homotritopic guest **1a** and Either Ester **2b** or Crowned Dendrons **3**−**5**, Designating the Enantiotopic Ethyleneoxy Protons Resulting from the Fact that the Two Faces of the Crown Ether Are Enantiotopic[b]

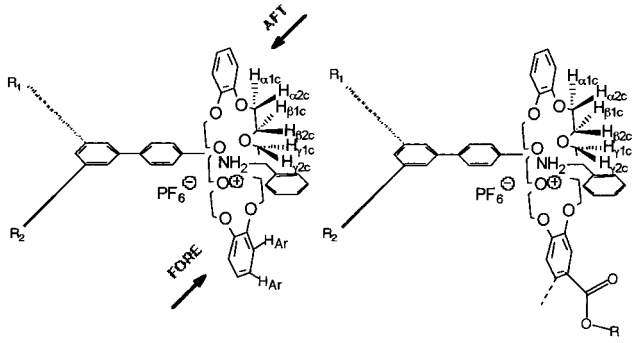

[a] When $R_1 = R_2$, as in [2]pseudorotaxane **7a** or [4]pseudorotaxane **9a** (Schemes 1 and 3), there are four of each type of proton. When $R_1 \neq R_2$ as in [3]pseudorotaxane **8a** (Schemes 1 and 4), the fore and aft pairs are enantiotopic if rotation of the crown ether about the ammonium ion and other rotations about biaryl bonds are slow. [b]There are in principle a minimum of 24 types of ethyleneoxy protons. An enantiomer of the structure shown results when the ester group occupies the position designated by the dashed line. In [3]pseudorotaxane **8** (Scheme 4), a racemic pair (*RR/SS*) and a third diastereomer (*RS*=*SR*) can form. In [4]pseudorotaxane **9** (Scheme 4), two racemic pairs (*RRR/SSS*) and (*RRS/SSR*) can form. Additionally, in [3]pseudorotaxanes **8** (Scheme 4), if rotation of the crown ether about the ammonium ion and other rotations about biaryl bonds are slow, there will be two geometric isomers, one with the the dendron units syn and one with them anti. In [4]pseudorotaxanes **9** (Scheme 4), under conditions of slow rotation there will be two geometric isomers: up−up−up = down−down−down and up−up−down = down−down−up with respect to the relative dispositions of the dendritic substitutent on the crown ether. All of these effects together produce complicated patterns for the ethyleneoxy proton signals.

Scheme 4. Designation of the Guest Protons in the [2]Pseudorotaxane Complexes **7**, [3]Pseudorotaxane Complexes **8**, and [4]Pseudorotaxane Complexes **9** from Homotritopic Guest **1a** and DB24C8 and Derivatives **3**−**5** for NMR Signal Assignments[a]

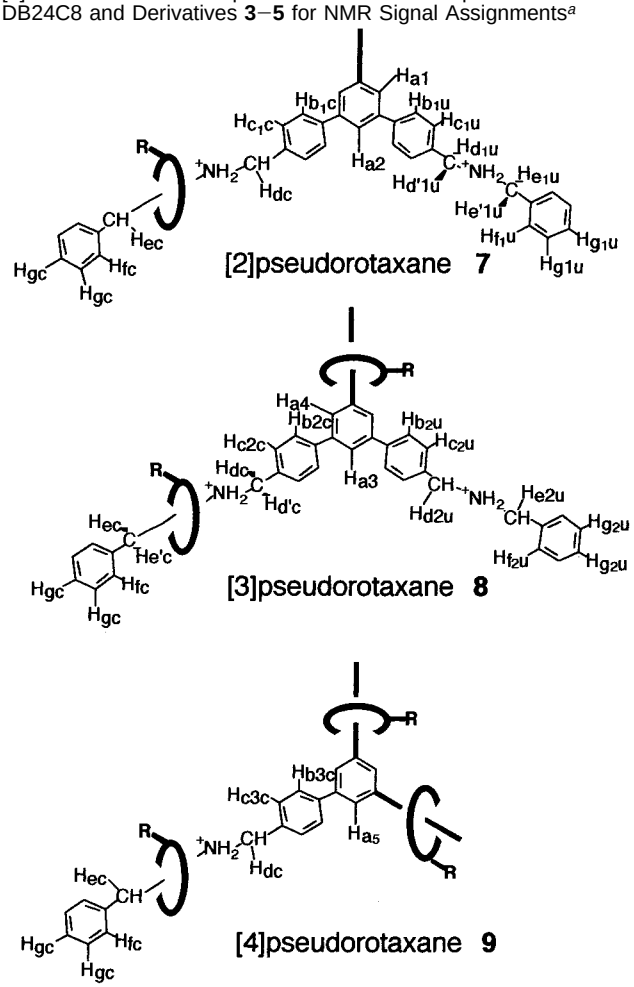

[a] With the exception of the protons on the central 1,3,5-substituted phenylene ring and the complexed NCH_2, the numbers in the subscripts refer to the stoichiometry of the complex, e.g., "1" for the 1:1 complex **7**. The letter following the number indicates whether the proton in question is associated with an uncomplexed arm ("u") or a complexed arm ("c"). (a, R = H (from DB24C8), b, R = $COOCH_3$ from **2b**, c, R = $COOCH_2G1$ from **3**, d, R = $COOCH_2G2$ from **4**, e, R = $COOCH_2G3$ from **5**).

plexed host (H_{Aru}). On the basis of integration of these signals, the fraction of complexed ammonium ion ranged from 26.1% at 10 mM DB24C8 to 96.4% at 50 mM. There is good agreement between the results from these signals and those from the NCH_2 peaks.

Turning to the aromatic protons of guest **1a**, proton H_{au} of the uncomplexed core **1a** is detected as a singlet at 7.94 ppm. As the concentration of DB24C8 is increased to 30 mM, a clear triplet (J = 1.2 Hz) emerges at 7.90 ppm due to H_{a1} of [2]-pseudorotaxane **7a** (Scheme 4), while the 7.94 ppm signal diminishes in intensity (Figure 1). As $[DB24C8]_o$ increases further to 40 mM, the former signal grows and the latter disappears, while a new triplet (J = 1.6 Hz) forms at 7.52 ppm, attributable to H_{a4} of [3]pseudorotaxane **8a** (Scheme 4). Further increases in $[DB24C8]_o$ lead to the appearance and dramatic increase in a singlet at 7.48 ppm due to H_{a5} of [4]pseudorotaxane **9a** (Scheme 4). Correspondingly, a doublet (J = 1.2 Hz) at 7.73 ppm ($[DB24C8]_o$ = 10−30 mM) is ascribed to H_{a2} of 1:1 complex **7a**, and the doublet (J = 1.6 Hz) at 7.69 ppm is attributed to H_{a3} of 1:2 complex **8a** (Scheme 4). The H_{a1} and H_{a2} signals are superimposed on the broad signal for complexed NH_2^+ at 7.62−7.75 ppm, the latter position in agreement with results for DB24C8/**3a** in CD_3CN.[19]

The phenylene protons of **1a** can be similarly analyzed as follows, even though there is a general upfield shift of all signals with increasing $[DB24C8]_o$. In the uncomplexed guest **1a**, H_{bu} is observed as a doublet (J = 8 Hz) at 7.58 ppm, and H_{cu} appears as a doublet (J = 8 Hz) at 7.88 ppm. Upon addition of DB24C8 (10 mM, Figure 1a), signals (doublets, J = 8 Hz) are observed

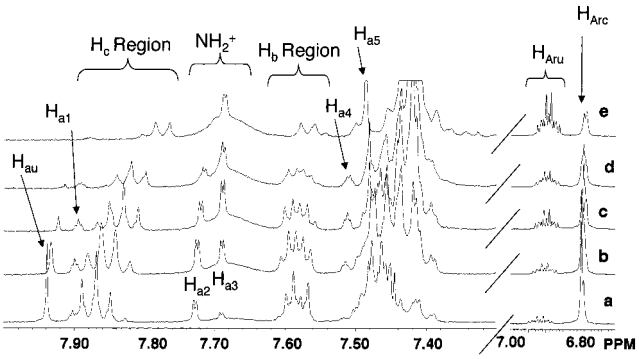

Figure 1. The aromatic region of ^1H NMR spectra (400 MHz, 22 °C) of CD_3CN solutions of homotritopic guest **1a** (10 mM) and DB24C8 (a) 10, (b) 20, (c) 30, (d) 40, (e) 90 mM. The first letter and the number of the subscript designate the proton (see Schemes 3 and 4) and the second letter whether the signal corresponds to uncomplexed (u) or complexed (c) species.

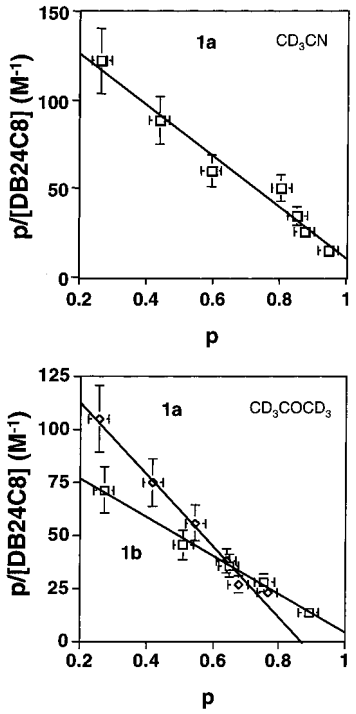

Figure 2. (a. Top): Scatchard plot for complexation of homotritopic guest **1a** and DB24C8 in CD_3CN at 22 °C ($y = -144x + 155$, $r^2 = 0.967$). (b. Bottom): Scatchard plots for complexation of DB24C8 with homotritopic guest **1a** (○) ($y = -168x + 146$, $r^2 = 0.987$) and deuterated homotritopic guest **1b** (□) in CD_3COCD_3 at 22 °C ($y = -90x + 95$, $r^2 = 0.994$). p = fraction of ammonium sites bound. Error bars in p, ±0.03 absolute; error bars in p/[DB24C8], ±15% relative.

at 7.57 and 7.59 (minor, ~1/3 intensity) ppm; we attribute the upfield signal at 7.57 ppm to H_{b1c} of [2]pseudorotaxane complex **7a** and the minor signal at 7.59 ppm to H_{b2c} (on a complexed arm) of [3]pseudorotaxane **8a** (Scheme 4). This region is complicated because complexes **7a**, **8a**, and **9a** each yield separate signals for their complexed arms. This is also the case for the uncomplexed arms of **7a** and **8a**, making accurate integration in this region impossible due to peak overlap. As $[DB24C8]_o$ increases, the doublet at 7.59 ppm grows in intensity at the expense of the 7.57 ppm signal, and at the same time a new doublet (J = 8 Hz) emerges at 7.56 and grows as $[DB24C8]_o$ increases. The final 7.56 ppm signal is attributed to H_{b3c} of [4]pseudorotaxane complex **9a** (Scheme 4, Figure 1e). The minor doublet (partially hidden) at 7.55 ppm for $[DB24C8]_o$ = 90 mM is attributed to H_{b2u} (uncomplexed arm) of residual [3]pseudorotaxane complex **8a** (Scheme 4, Figure 1e); both the NCH_2 and DB24C8 aromatic signals indicate that >95% of the NH_2^+ units are complexed at this concentration.

In the case of the H_{cu} signal (7.88 ppm) of homotritopic guest **1a**, the changes are analogous, producing doublets, all with J = 8 Hz, with chemical shifts of ~7.84, ~7.86, and ~7.88 ppm (Figure 1, all move upfield with increasing $[DB24C8]_o$). As $[DB24C8]_o$ increases from 10 to 90 mM, the 7.88 ppm peak disappears, leaving two overlapping doublets (J = 8 Hz) at 7.84 (major) and 7.86 (minor) ppm. These signals are assigned as follows: 7.84 ppm, H_{c3c} of [4]pseudorotaxane **9a**; 7.86 ppm, H_{c2c} of [3]pseudorotaxane **8a**; 7.88 ppm, H_{c1c} of [2]pseudorotaxane **7a** (Scheme 4). Note the symmetry of the residual signals at 7.78 and 7.56 ppm, respectively, representing H_{c3c} and H_{b3c} of **9a** with minor peaks due to H_{c2c} and H_{b2c} of **8a** (Scheme 4) at $[DB24C8]_o$ = 90 mM (Figure 2e).

The ortho, meta, and para protons H_{fu} and H_{gu} of the terminal phenyl groups of uncomplexed **1a** appear at 7.48 ppm. As reported for DB24C8 and **6a** in CD_3CN,[19] a new signal appears at 7.26 ppm upon addition of DB24C8 to **1a** (not shown). The pattern does not change as $[DB24C8]_o$ increases from 10 to 90 mM; furthermore, the ratio relative to the aromatic protons (8H) of complexed DB24C8 at 6.8 ppm is constant (0.38). We conclude that this signal is due to the three complexed terminal phenyl protons H_{gc} of species **7a**, **8a**, and **9a** (Scheme 4) and is part of a coupling pattern, the rest of which (H_{fc}) is hidden inside the multiplet at 7.35−7.55 ppm, as also reported for DB24C8/**6a** in CD_3CN.[19]

With these assignments[21] in hand, it is possible to estimate the three association constants K_1, K_2, and K_3 (Scheme 1) by several corroborative methods. First, using the extent of complexation, p, determined from the NCH_2 and crown ether signals, a Scatchard plot was constructed (Figure 2a). The linearity of this plot indicates conclusively that the complexation sites act independently.[22] Furthermore, the slope of this plot is proportional to the negative of the average association constant (K_{ave}), and the intercept is K_{ave} (eq 1).[22] Because the three guest sites act independently, the ratios of the association constants are known from statistics to be 3:1:1/3,[22] meaning all K values can be determined (Table 1).

$$p/[DB24C8] = -pK_{ave} + K_{ave} \qquad (1)$$

where p is the fraction of NH_2^+ sites of **1a** bound, and K_{ave} is the average microscopic association constant.

Direct estimates of K_1, K_2, and K_3 are available from the signals for H_{au}, H_{a1}, and H_{a4}, which give the concentrations of **1a**, [2]pseudorotaxane **7a**, and [3]pseudorotaxane **8a**. Unfortunately, the H_{a5} signal of [4]pseudorotaxane **9a**, though observable, is not easily integrated. However, the concentration of **9a** can be determined by realizing that $N_{\mathbf{1a}} + N_{\mathbf{7a}} + N_{\mathbf{8a}} + N_{\mathbf{9a}} = 1$, where N represents the mole fraction of each species. The total integral from 7.1 to 8.0 ppm represents a total of 30 aromatic protons plus the protons of the complexed NH_2^+ moieties of the core structure **1a**. Therefore, $N_{\mathbf{1a}} = \#H_{au}/3$, $N_{\mathbf{7a}} = \#H_{a1}$, and $N_{\mathbf{8a}} = \#H_{a4}/2$; $N_{\mathbf{9a}}$ was estimated by difference. Furthermore, the percent complexation was independently checked for the crown ether versus the NCH_2 moieties. These K values (Table 1) are in reasonable agreement with the values derived from the Scatchard treatment, but somewhat higher. Generally, we have observed that K decreases with $[DB24C8]_o$ in these systems; possible reasons for this are discussed below. Because the Scatchard plot includes all the concentrations, it yields a lower average K than direct determinations at lower concentrations. K_{ave} (1.5×10^2 M^{-1}) is lower than the value of 420 M^{-1} reported for complexation of dibenzylammonium hexafluorophosphate (**6a**) and DB24C8 in CD_3CN.[19] Because if all else were equal the average K value for **1a** would be the same as the K value for **6a**/DB24C8, it seems that binding of the crown ether to the guest units of homotritopic **1a** is less favored than its binding to **6a**. We attribute this partially to an

(22) Freifelder, D. M. *Physical Biochemistry*; W. H. Freeman and Co.: New York, 1982; pp 659−660. Marshall, A. G. *Biophysical Chemistry*; Wiley and Sons: New York, 1978; pp 70−77. Connors, K. A. *Binding Constants*; Wiley and Sons: New York, 1987; pp 78−86.

Table 1. Association Constants for Model Psuedorotaxane Complexes, 22 °C

host/guest system	solvent	$10^{-2} \times K_1$ (M^{-1})	$10^{-2} \times K_2$ (M^{-1})	$10^{-2} \times K_3$ (M^{-1})	$10^{-6} \times K_o$[a] (M^{-3})
DB24C8/**1a**	CD_3CN	4.4 (±0.1)[b]	1.4 (±0.2)[b]	0.41 (±0.04)[b]	2.5 (±0.7)[c]
		3.1 (±0.4)[d]	1.0 (±0.2)[d]	0.35 (±0.04)[d]	1.1 (±0.6)[c]
DB24C8/**1a**	CD_3COCD_3	3.7 (±1.7)[e]	1.3 (±0.2)[e]	0.57 (±0.13)[e]	2.7 (±2.4)[c]
		3.3 (±0.5)[f]	1.1 (±0.2)[f]	0.37 (±0.05)[f]	1.3 (±0.6)[c]
		7.3 (±1.3)[g]	2.2 (±0.9)[g]	0.48 (±0.14)[g]	7.7 (±7.0)[c]
DB24C8/**1b**	CD_3COCD_3	1.9 (±0.3)[h]	0.64 (±0.10)[h]	0.21 (±0.04)[h]	1.7 (±0.7)[c]
DB24C8/**6a**	CD_3COCD_3	3.2 (±0.2)[i]			
2b/**6a**	CD_3COCD_3	2.0 (±0.1)[j]			
DB24C8/**6b**	CD_3COCD_3	1.8 (±0.1)[k]			
DB24C8/**1a**	$CDCl_3$			3.9 (±0.4)[l]	

[a] Overall association constant for formation of [4]pseudorotaxane **9a** from 1 mol of **1a** or **1b** and 3 mol of DB24C8; $K_o = K_1K_2K_3$. [b] Relative concentrations were estimated by integration of H_a signals for free **1a** (7.94 ppm, H_{au}, 3H), [2]- (**7a**, 7.90 ppm, H_{a1}, 1H), and [3]-pseudorotaxanes (**8a**, 7.52 ppm, H_{a4}, 1H); [4]-pseudorotaxane (**9a**) concentration was determined by difference using values of extent of complexation estimated from both complexed and "uncomplexed" NCH_2 and crown ether aromatic protons, which also yielded the concentration of the "uncomplexed" crown ether. Range of initial concentrations of **1a**/DB24C8 used: for K_1, 10/10 to 10/60 mM; for K_2, 10/20 to 10/60 mM/mM; for K_3, 10/30 to 10/60 mM. Error bars are standard deviations from multiple independent integrations of the spectra. [c] Error cited is average deviation from the nominal value calculated using both the maximum and the minimum values for K_1, K_2, and K_3 based on the individual error bars. [d] By Scatchard plot analysis (Figure 2a) using values of extent of complexation estimated from both complexed and "uncomplexed" NCH_2 and crown ether aromatic protons, which also yielded the concentration of the "uncomplexed" crown ether, over the range of initial concentrations of **1a**/DB24C8 from 10/10 to 10/90 mM/mM. $K_{ave} = (-\text{slope} + \text{intercept})/2 = 1.5 \times 10^2\ M^{-1} = 4.33K_3$; $K_2 = 3K_3$ and $K_1 = 9K_3$. Error bars are based on maximum and minimum slope fits. [e] The molar ratios of **1a**, **7a**, **8a**, and **9a** were determined by integration of H_{au} (7.96 ppm, 3H, **1a**), H_{a1} (7.94 ppm, 1H, **7a**), H_{a2} (7.82 ppm, 2H, **7a**), H_{a3} (7.80 ppm, 2H, **8a**), and H_{a5} (7.67 ppm, 3H, **9a**) (Scheme 4). The signals were integrated by the cut and weigh method, taking into account the facts that H_{a2} and H_{a3} ride atop the signal for complexed NH_2^+ and that H_{a4} overlaps H_{a5}. In the former case, the baseline was corrected, and in the latter, since both H_{a3} and H_{a4} are derived from **8a**, by subtraction of one-half the integral of H_{a3}. The concentration of uncomplexed DB24C8 was determined by integration of the well resolved H_{bc} (3.91 ppm) versus H_{bu} (3.83 ppm) (Scheme 2). The results from the following initial concentrations of **1a**/DB24C8 were used to evaluate K_1, 10/20, 10/20, 10/30 mM/mM; K_2, 10/30, 10/40, 10/50, 10/60 mM/mM; K_3, 10/20, 10/30, 10/40, 10/50, 10/60 mM/mM. Error bars are the standard deviations. [f] By Scatchard plot analysis (Figure 2b) using values of extent of complexation estimated from both complexed and "uncomplexed" NCH_2 and β-OCH_2 signals, which also yielded the concentration of the "uncomplexed" crown ether, over the range of initial concentrations of **1a**/DB24C8 from 10/10 to 10/90 mM/mM. $K_{ave} = (-\text{slope} + \text{intercept})/2 = 1.6 \times 10^2\ M^{-1} = 4.33K_3$; $K_2 = 3K_3$ and $K_1 = 9K_3$. Error bars are based on maximum and minimum slope fits. [g] By deconvolution of "uncomplexed" NCH_2 signals to determine the relative concentrations of **1a**, [2]- (**7a**), and [3]-pseudorotaxanes (**8a**); the extent of complexation was estimated from both complexed and "uncomplexed" NCH_2 and β-OCH_2 signals, which also yielded the concentration of the "uncomplexed" crown ether. The concentration of the [4]pseudorotaxane (**9a**) was determined by difference. The results from solutions of the following initial concentration ranges of **1a**/DB24C8 were used: for K_1, from 10/10 to 10/60 mM/mM; for K_2, from 10/10 to 10/60 mM/mM; for K_3, from 10/30 to 10/60 mM/mM. Error bars are standard deviations. [h] By Scatchard plot analysis (Figure 2b) using values of extent of complexation estimated from both complexed and "uncomplexed" NCH_2 and β-OCH_2 signals, which also yielded the concentration of the "uncomplexed" crown ether, over the range of initial concentrations of **1b**/DB24C8 from 10/10 to 10/90 mM/mM. $K_{ave} = (-\text{slope} + \text{intercept})/2 = 93\ M^{-1} = 4.33K_3$; $K_2 = 3K_3$ and $K_1 = 9K_3$. Error bars based on maximum and minimum slope fits. [i] By integration of complexed versus "uncomplexed" NCH_2 and γ-OCH_2 signals at initial concentrations of **6a**/DB24C8 = 20/20 mM/mM. [j] By integration of H_{dc} versus H_{du} signals at initial concentrations of **2b**/**6a** = 20.4/20.3 mM/mM. [k] By integration of complexed versus "uncomplexed" NCH_2 signals over a range of initial concentrations of **6b**/DB24C8 from 10/10 to 10/60 mM/mM. [l] By integration of H_{c2u} and H_{b2u} of [3]pseudorotaxane **8a** versus H_{c3c} and H_{b3c} of [4]pseudorotaxane **9a** (Scheme 4), respectively, in a solution initially 30 mM in DB24C8 containing solid **1a** in an amount equivalent to 10 mM had it all dissolved; 90.0 ± 0.5% of the solid dissolved.

unaccounted equilibrium process that competes more strongly with pseudorotaxane formation in the case of **1a** (see below).

B. In CD_3COCD_3. 1. Tritopic Guest 1a with DB24C8. The aliphatic region of the ^1H NMR spectra of solutions of the homotritopic molecule **1a** and DB24C8 in acetone-d_6 (Figure 3) again reveals slow association and dissociation. The signal assignments were made with the aid of the COSY spectrum.[21] In CD_3CN the ethyleneoxy proton signals were not readily integrated individually, whereas in CD_3COCD_3 the signals for the complexed and uncomplexed β-protons, in particular, are observed with baseline separation, allowing facile quantitation of the fraction of crown ether involved in complexation.

Peaks in the aromatic region of the ^1H NMR spectra of solutions of **1a** and DB24C8 were assigned by COSY (Figure 4) and analogy to CD_3CN spectra: H_{au} of **1a** at 7.98 ppm, H_{a1} of [2]pseudorotaxane **7a** at 7.94 ppm, H_{a2} of **7a** at 7.73 ppm, H_{a3} of [3]pseudorotaxane **8a** at 7.69 ppm, and H_{a5} of [4]-pseudorotaxane **9a** at 7.66 ppm (Scheme 4). The H_{gc} signal for pseudorotaxanes **7a**, **8a**, and **9a** (Scheme 4) at 7.3 ppm is well resolved; comparing its integral with that for the total aromatic proton resonances of the crown ether (6.8−7.0 ppm) allows an independent assessment that agrees well with results from the β-OCH_2 and NCH_2 signals.

An intriguing observation in the ^1H NMR spectra of solutions of **1a** and DB24C8 is the behavior of the signals for H_{du} and H_{eu} (Figure 3). Two sharp singlets corresponding to H_{du} and H_{eu} beginning at 4.64 and 4.58 ppm in **1a** shift upfield and disintegrate into broader multiplets with increasing concentration of DB24C8 and eventually disappear with 9 equiv of DB24C8. The behavior of the signals for H_{du} and H_{eu} is partially attributable to the existence of the [2]- and [3]-pseudorotaxane complexes **7a** and **8a**. As illustrated in Scheme 4, when one of the arms is occupied with DB24C8, the initially equivalent pairs of H_{eu} and H_{du} protons of **1a** each become nonequivalent (diastereotopic) in **7a**, meaning that there are two pairs of nonequivalent benzylic protons, H_{d1u}, $H_{d1'u}$, H_{e1u}, and $H_{e1'u}$, on each uncomplexed arm. When two of the arms are complexed with DB24C8 in **8a**, the two H_{du} protons and two H_{eu} protons of **8a** are once again equivalent by symmetry as shown.

The gradual upfield shifts observed for H_{du} and H_{eu} signals were initially hypothesized to be the result of the increased concentration of "free" PF_6^- with respect to the concentration of uncomplexed ammonium salt moieties, that is, ion pairing of the "free" PF_6^- with the uncomplexed ammonium species. The pseudorotaxane geometry does not allow tight ion pairing, so the "free" PF_6^- ions resulting from complexation are potentially available to interact with uncomplexed ammonium ion moieties, as we had previously observed in a paraquat-based pseudorotaxane system.[23] However, addition of *n*-Bu_4NPF_6 in concentrations up to 2 M to 10 mM solutions of **1a** (without

(23) Yamaguchi, N.; Nagvekar, D. S.; Gibson, H. W. *Angew. Chem., Int. Ed.* **1998**, *37*, 2361−2364.

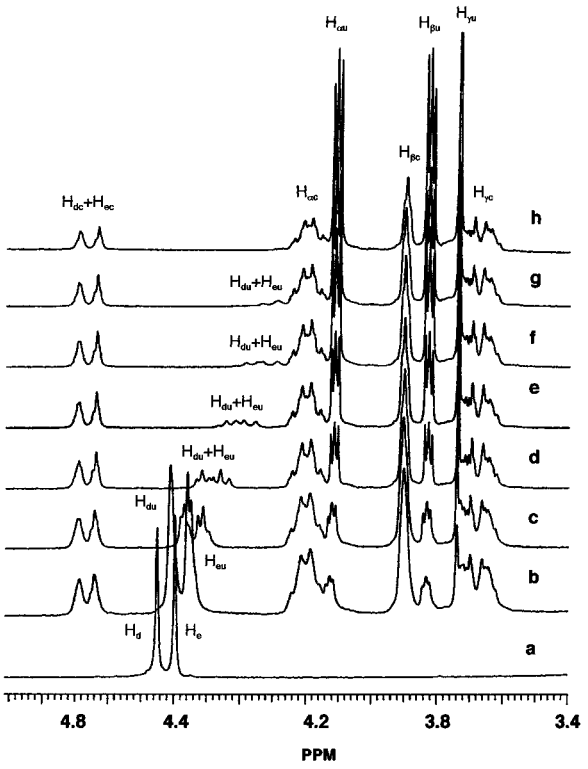

Figure 3. The aliphatic region of ^{1}H NMR spectra (400 MHz, 22 °C) of CD_3COCD_3 solutions of homotritopic guest **1a** (10 mM) and DB24C8 (a) 0, (b) 10, (c) 20, (d) 30, (e) 40, (f) 50, (g) 60, and (h) 90 mM. The first letter and number of the subscript designate the proton (see Schemes 3 and 4) and the second letter whether the signal corresponds to uncomplexed (u) or complexed (c) species.

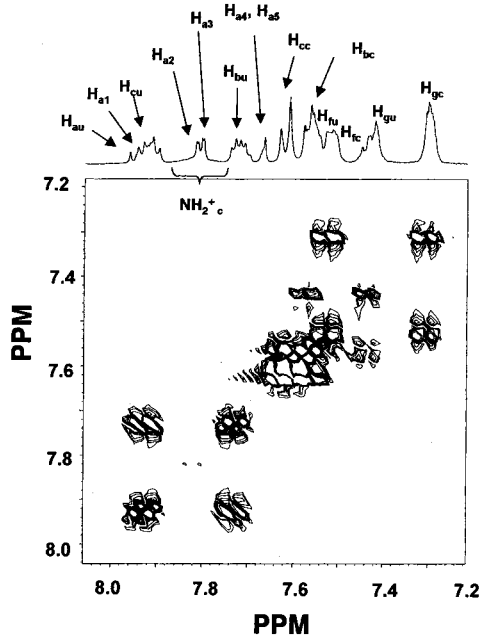

Figure 4. Aromatic region of COSY spectrum of a CD_3COCD_3 solution of homotritopic guest **1a** (10 mM) and DB24C8 (30 mM). The first letter and number of the subscript designate the proton (see Scheme 4) and the second letter whether the signal corresponds to uncomplexed (u) or complexed (c) species.

DB24C8) had *no* effect on the chemical shifts for H_{du} and H_{eu}. Furthermore, low-temperature NMR spectroscopy on a solution of **1a**/DB24C8 (10/30 mM)[24] did not reveal any change in the chemical shifts of H_{du} and H_{eu}. These results indicate that ion pairing is not the source of the observed shifts.

2. Monotopic Deuterated Guest 6b and DB24C8. To gain further insight into these signal pattern changes for H_{du} and H_{eu}, deuterated dibenzylammonium hexafluorophosphate **6b** was prepared,[21] and its complexation was examined. As $[DB24C8]_o$ was increased from 0 to 140 mM in a solution 10 mM in **6b**, the signal for the uncomplexed NCH_2 moved upfield 0.05 ppm as compared to 0.3 ppm for **1a** in Figure 3. The ^{31}P resonance did not change, and ^{19}F chemical shift changes were relatively small (<0.5 ppm). These results argue against ion pairing of the PF_6 anions "freed" by the complexation with the accessible uncomplexed sites.

3. Tritopic Deuterated Guest 1b and DB24C8. The ^{1}H NMR spectrum of deuterated homotritopic molecule **1b**[21] in acetone-d_6 revealed the signal for the H_d proton at 4.58 ppm, the same position as in **1a**. In spectra of solutions of guest **1b** and DB24C8,[21] the signal for H_{du} did not shift upfield as dramatically or change its shape with increased concentration of DB24C8 as we observed with protiated analogue **1a** (Figure 3)!

To explain why the NCH_2 signals in completely uncomplexed **1a** are shifted and why discrete signals for **1a**, **7a**, and **8a** are not observed at specific fixed chemical shifts, we propose nonpseudorotaxane complexation of the unthreaded NCH_2^+ moieties, that is, of the exo type, either "perching" or "nesting",[25] which is well known.[26] Thus, as the crown ether concentration is increased, the fraction of ammonium ion moieties that are involved in this latter type of complexation also increases. Because this equilibration is rapid on the NMR time scale, the signals are time-averaged. The increased electron density on the NH_2^+ moieties as a result of this H-bonding and also the shielding effect of the benzo groups of the proximal crown ether cause an upfield shift of the NCH_2 protons. In the deuterated homotritopic **1b** there are only H_d protons; the deuterons on the "external" benzylic positions are less acidic than the H_d protons,[27] and this apparently prohibits, or at least inhibits, formation of the exo complexes and/or alters the co-conformations of the pseudorotaxane moieties in such a way that no chemical shift change results from increased [DB24C8].

4. Homotritopic Guest 1a and Dibenzo-18-crown-6. For evidence in support of exo complexation, homotritopic guest **1a** (10 mM) was examined in acetone-d_6 in the presence of 30 mM dibenzo-18-crown-6 (DB18C6), which is too small to form a pseudorotaxane. Indeed, in accordance with the hypothesis of formation of exo hydrogen bonded complexes, the NCH_2 protons shifted upfield by 0.05 ppm. However, with deuterated dibenzylammonium hexafluorophosphate **6b** there were no signficant changes in the chemical shifts of the NCH_2 protons. Protiated analogue **6a** (20 mM) in the presence of DB18C6 (saturated, <10 mM) also revealed a small upfield shift; the

(24) Below −40 °C all of the crown ether was consumed based on the β-proton signals. Because of the lack of resolution of appropriate signals for **1**, **7a**, **8a**, and **9a**, it was not possible to estimate K_1, K_2, and K_3.

(25) Newcomb, M.; Moore, S. S.; Cram, D. J. *J. Am. Chem. Soc.* **1977**, *99*, 6405−6410.
(26) Metcalfe, J. C.; Stoddart, J. F.; Jones, G. *J. Am. Chem. Soc.* **1977**, *99*, 8317−8319. Izatt, R. M.; Lamb, J. D.; Izatt, N. E.; Rossiter, B. E., Jr.; Christensen, J. J.; Haymore, B. L. *J. Am. Chem. Soc.* **1979**, *101*, 6273−6276. Doxsee, K. M.; Francis, P. E., Jr.; Weakley, T. J. R. *Tetrahedron* **2000**, *56*, 6683−6691 and references therein.

(27) For a comparison of the acidity of H_2O versus D_2O (pK_a = 15.4 and 17.2, respectively, at 25 °C in H_2O) see: Isaacs, N. *Physical Organic Chemistry*, 2nd ed.; Longman Scientific and Technical: Essex, U.K., 1995; p 244.

lower saturation concentration of DB18C6 in a solution of ammonium salt **6a** relative to that in triammonium salt **1a** (~40 mM) is consistent with stronger exo complexation of **1a**, possibly due to its higher charge density and opportunities for multisite H-bonding and other attractive interactions, for example, π-stacking. It should be noted that the extent of exo complexation with DB18C6 is expected to be lower than with DB24C8 since the latter possesses twice as many nonphenolic ether oxygen atoms which are more basic than the phenolic ether oxygen atoms.

A significant aspect of the formation of exo complexes is that the "free" ammonium ion and crown ether moieties are consumed, thereby reducing the true concentrations of both species. Therefore, the calculated association constants are underestimated. The formation of exo hydrogen bonded complexes nicely rationalizes both the shifts of "uncomplexed", that is, nonpseudorotaxane type, benzylic NCH_2 protons (and other signals), and the decrease in calculated *K* values with increasing concentration of host moieties.

5. Association Constants of Homotritopic Guests 1a and 1b with DB24C8. The association constants for the pseudorotaxane complexes of **1a** and DB24C8 in acetone-d_6 were first estimated via the Scatchard treatment (Figure 2b, Table 1) based on integration of the complexed and "uncomplexed" NCH_2 and crown ether signals. Because the plot is linear, binding is noncooperative, that is, statistical. Similarly, the association constants for the pseudorotaxane complexes of deuterated homotritopic guest **1b** and DB24C8 in acetone-d_6 were estimated via the Scatchard treatment (Figure 2b, Table 1). The lower association constants for **1b** as compared to those of **1a** are presumably due to the lower acidity[27] of the benzylic deuterons of the ammonium salt moieties in **1b** relative to the protons of **1a**, since CH- -O bonding is known to be important in these systems.[19] Note that again the average *K* value (1.6×10^2 M^{-1}) for **1a**/DB24C8 is less than the value for monotopic guest **6a** with DB24C8 (Table 1); we attribute this partially to the greater propensity of tritopic **1a** to participate in exo complexation relative to the simpler guest **6a**. This could be due to simultaneous bonding to more than one NH_2^+ site and/or the increased possibilities for attractive interactions of the aromatic rings of the host and guest **1a**, coupled with screening of the three proximate ionic charges.

A second analysis was based on direct integration of the signals for H_{au} of **1a**, H_{a2} of **7a**, H_{a3} of **8a**, and H_{a5} of **9a**. The *K* values agree well with those derived from the Scatchard plot (Table 1), but as noted above are slightly higher.

A third analysis involved the "uncomplexed" (actually time-averaged uncomplexed and exo complexed) benzylic protons of homotritopic guest **1a**, that is, H_{du} and H_{eu} (Figure 3). We assigned the three pairs of signals for these protons in **1a**, [2]-pseudorotaxane **7a**, and [3]pseudorotaxane **8a**. The three species revealed different peak separations for H_{du} and H_{eu}, but the pairs were easily identified because the intensities of the two peaks in each pair were by definition identical. The signals were deconvoluted to provide three distinct pairs of peaks which were integrated to estimate the relative amounts of **1a**, **7a**, and **8a**. The relative amount of [4]pseudorotaxane **9a** could then be estimated as outlined above by difference, based on the percentage of **1a** that had been complexed as deduced from the relative integrals for $H_{dc} + H_{ec}$ versus $H_{du} + H_{eu}$ and confirmed by integration of the crown ether aromatic signals (6.8−7.0 ppm) and that of H_{gc} of pseudorotaxanes **7a**, **8a**, and **9a** (Scheme 4) at 7.3 ppm. The *K*'s (Table 1) are close to the relative, statistical values (3:1:$^1/_3$) anticipated for independent guest sites in the homotritopic species,[22] but somewhat higher, particularly for K_1, than those resulting from the Scatchard plot. The reason for this lies in the concentration dependence of the *K* values; the Scatchard plot gives an average value over the entire concentration range of DB24C8, while the integration technique was used only at lower $[DB24C8]_o$.

The K_a for [2]pseudorotaxane formation from DB24C8 with deuterated **6b** is ca. one-half that with protiated **6a** (Table 1). Variable temperature (+22 to −60 °C) ^1H NMR spectroscopy on a solution of DB24C8/**6a** produced results similar to those reported for this system in CD_3CN, showing some curvature in a van't Hoff plot.[19b] Although this has been attributed to "a nonneglible heat capacity($\Delta C°_p$)",[19b] we suggest that it is due to the fact that the association constants for pseudorotaxane formation are underestimated to differing extents at different temperatures due to the fact that the exo complexation and pseudorotaxane complexation do not have the same temperature dependence; recall that the concentrations of the uncomplexed host and guest species (here DB24C8 and **6a**) have been assumed to include all species not in the pseudorotaxane state, thereby failing to take into account exo complexation. The *K* values are thereby underestimated.

6. 2-Carbomethoxydibenzo-24-crown-8 (2b) with Dibenzylammonium Hexafluorophosphate (6a). 2-Carbomethoxydibenzo-24-crown-8 (**2b**) serves as a good model for dendrons **3**−**5**. Upon complexation with **6a**,[21] the H_{dc} and H_{du} signals are well resolved, providing one means of assessing the extent of complexation. The integrals for the well-resolved complexed versus uncomplexed γ-protons (Schemes 2 and 3b) provide a second independent estimate of the extent of complexation. The signal for the complexed γ-protons reveals more than one type of environment (Scheme 3b). The association constant for [2]-pseudorotaxane formation from ester **2b** and **6a** was lower than that for DB24C8 with **6a** (Table 1), as expected because of the electron-withdrawing effect of the ester moiety.[19f]

C. In $CDCl_3$. 1. Tritopic Guest 1a with DB24C8. Figure 5 shows the ^1H NMR spectrum of a $CDCl_3$ solution of DB24C8 (30 mM) and homotritopic core molecule **1a** (as a solid in an amount that corresponded to 10 mM had it completely dissolved). Note that **1a** is not soluble in $CDCl_3$. Again the exchange process is slow.

In contrast to spectra in acetone-d_6, there is only one set of NCH_2 signals. We initially concluded,[18] therefore, that all of the homotritopic ammonium salt **1a** in solution was completely complexed; that is, only [4]pseudorotaxane **9a** and DB24C8 were present. However, careful integration indicated that <100% of the ammonium ion moieties of **1a** were complexed in these solutions. This conclusion was reached on the basis of two analyses. In the first analysis, the region from 4 to 4.3 ppm revealed an excess of protons over the expected eight from α-OCH_2 moieties when compared to the aromatic proton signals of the crown ether (6.76−6.95 ppm). From this "excess" integral, attributed to uncomplexed NCH_2, and that for the complexed NCH_2 signal at 4.6−4.7 ppm, we found that 89.5% of the NH_2^+ units were complexed and 10.5% uncomplexed at $[DB24C8]_o = 30$ mM. By analogy to the CD_3CN spectra, the

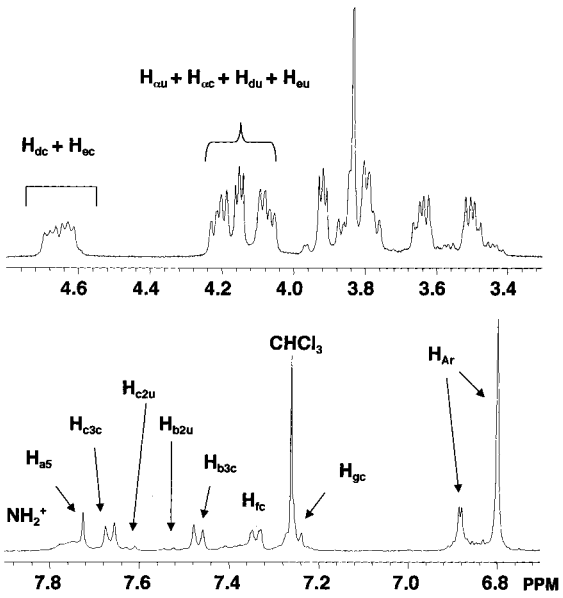

Figure 5. The ^{1}H NMR spectrum (400 MHz, 22 °C) of a 30 mM $CDCl_3$ solution of DB24C8 mixed with $^1/_3$ mol equiv of solid tritopic guest **1a** after 18 h. The first letter and number of the subscript designate the proton (see Schemes 3 and 4) and the second letter whether the signal corresponds to uncomplexed (u) or complexed (c) species.

small doublets at 7.62 and 7.53 ppm were assigned to H_{c2u} and H_{b2u} of [3]pseudorotaxane **8a**, respectively, and the major doublets at 7.67 and 7.47 ppm to H_{c3c} and H_{b3c} of [4]-pseudorotaxane **9a** (Scheme 4), respectively. In the second analysis, integration of the well-resolved signals at 7.53 and 7.47, using the crown ether aromatic proton signal integral as a reference, indicated at $[DB24C8]_o = 30$ mM that 9.4% of the dissolved **1a** was present as [3]pseudorotaxane **8a** and 90.6% as [4]pseudorotaxane **9a**. The results from the two analyses are in excellent agreement, allowing K_3 to be determined (Table 1). Thus, a small percentage of [2]pseudorotaxane **7a** must exist in these $CDCl_3$ solutions, although it was not detected.

While it is not possible to determine the first two association constants in this solvent, the amount of homotritopic guest **1a** that dissolved was determined from the integrals noted above; 91 ± 1% of the solid **1a** dissolved in 30 mM DB24C8, producing a 9.1 ± 0.1 mM total concentration of **1a**-based species, that is, [3]pseudorotaxane **8a**, and [4]pseudorotaxane **9a**.

2. 2-Carbomethoxydibenzo-24-crown-8 (2b) with Homotritopic Guest 1a. Complexation was evidenced by the ^{1}H NMR spectrum[21] of a 15 mM $CDCl_3$ solution of 4-carbomethoxydibenzo-24-crown-8 (**2b**) with solid **1a** in an amount which if dissolved corresponded to 5.0 mM. After 22 h, 73.1% of the solid **1a** had dissolved ($[\mathbf{1a}]_{total} = 3.65$ mM), and the NH_2^+ moieties were 83% complexed as determined from the integrals of the $H_{dc} + H_{ec}$ signals at 4.6−4.8 versus the $H_{du} + H_{eu}$ peaks at 4.25−4.35 ppm and the integral of all of the OCH_2 signals of the crown ether.

3. Third Generation Dendron 5 with Dibenzylammonium Hexafluorophosphate (6a). ^{1}H NMR spectra of a 10 mM solution of third generation dendron **5** in chloroform-*d* mixed with 1 mol equiv of solid dibenzylammonium hexafluorophosphate (**6a**) were recorded periodically; no changes were noted over a 24 h period (Figure 6). The signals for the benzylic protons H_n, H_q, and H_t of dendron **5** (Scheme 2) in the [2]pseudorotaxane complex **5**:**6a** were not distinguishable from

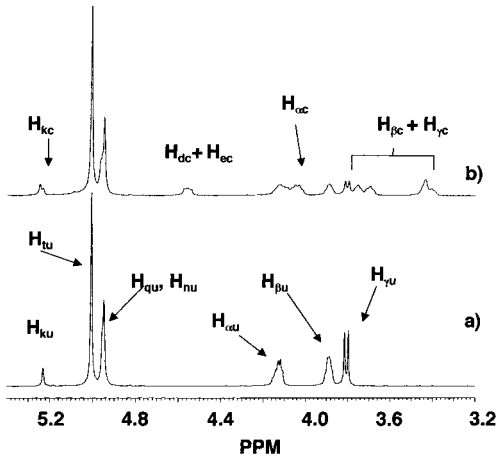

Figure 6. The aliphatic region of ^{1}H NMR spectra (400 MHz, 22 °C) of (a) a 10 mM $CDCl_3$ solution of third generation dendron **5** and (b) a 10 mM $CDCl_3$ solution of third generation dendron **5** mixed with 1 mol equiv of solid monotopic guest **6a**. The first letter and number of the subscript designate the proton (see Schemes 2 and 4) and the second letter whether the signal corresponds to uncomplexed (u) or complexed (c) species.

Table 2. Supramolecular Formulas, Calculated Supramolecular Weights, and Observed (Ms) Mass/Charge Ratios

structure	molecular formula	calcd MW	obs *m/z*
9a-PF_6	$[C_{48}H_{48}N_3P_2F_{12}(C_{24}H_{32}O_8)_3]^+$	2300.9	2300.5[a1,b]
8a-$2PF_6$	$[C_{48}H_{48}N_3PF_6(C_{24}H_{32}O_8)_2]+$	1707.8	1707.8[a2]
7a-PF_6-HPF_6	$[C_{48}H_{47}N_3PF_6(C_{24}H_{32}O_8)]+$	1258.6	1258.6[a3]
7a-PF_6-$2HPF_6$	$[C_{48}H_{46}N_3(C_{24}H_{32}O_8)]+$	1112.6	1112.6 [a4]

[a] FAB mass spectrum recorded in the positive ion mode using 3-nitrobenzyl alcohol (3-NBA) as the matrix; sample prepared by slow evaporation (25 °C) of an acetone solution 10 mM in **1a** and 30 mM in DB24C8. (1) 4%, (2) 33%, (3) 5%, (4) 11% of base peak at $m/z = 471.2$ $(DB24C8 + Na)^+$. [b] High-resolution FAB: 2300.9452 $(M)^+$, 2301.9493 $(M + 1)^+$, 2303.9608 $(M + 2)^+$ in relative intensities 71:100:73; calcd 2300.9423 $(M)^+$, 2301.9457 $(M + 1)^+$, 2303.9614 $(M + 2)^+$ in relative intensities 75:100:69.

those of uncomplexed **5**, nor were there changes in the aromatic proton signals of the third generation dendron. However, shifts of the signals for benzylic ether protons H_k and the ethyleneoxy protons were observed, but no uncomplexed NCH_2 (H_{du}) signal could be detected. The total concentration of **6a** was 5.59 mM based on the integral of the 4.55 ppm signal for $H_{dc} + H_{ec}$ (4H per **6a**) versus that of all of the benzylic proton signals H_k, H_n, H_q, and H_t (30H per **5**). All of **6a** was present in solution as the [2]pseudorotaxane complex.

D. Mass Spectrometry. The FAB MS spectrum exhibited signals corresponding to the [4]pseudorotaxane complex **9a** after the loss of a PF_6^- counterion, the [3]pseudorotaxane complex **8a** with only one PF_6^- counterion, and the [2]pseudorotaxane complex **7a**, both intact and after loss of PF_6^-.[21] The presence of [4]pseudorotaxane **9a** was confirmed by high-resolution FAB MS (Table 2).

III. Dendrimer Self-Assembly: Tritopic Guest 1a with First, Second, and Third Generation Dendrons 3−5. A. In CD_3COCD_3. ^{1}H NMR spectra of solutions of **1a** with first (Figure 7), second,[21] and third (Figure 8) generation dendrons **3**, **4**, and **5** individually in acetone-d_6 exhibit signals for complexed and free moieties due to slow association and dissociation. The signals for H_{du} and H_{eu} of **1a** (singlets at 4.64 and 4.58 ppm) gradually shifted upfield and changed their shapes to give multiple peaks, while their intensity decreased as the

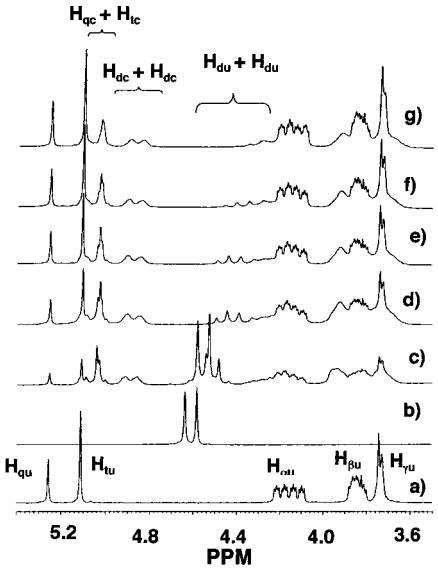

Figure 7. The aliphatic region of ^{1}H NMR spectra (400 MHz, 22 °C) of CD_3COCD_3 solutions of homotritopic guest **1a** and first generation monotopic dendron **3** at (a) 0/10, (b) 10/0, (c) 10/10, (d) 10/30, (e) 10/40, (f) 10/50, and (g) 10/60 mM initial concentrations. The first letter of the subscript designates the proton (see Schemes 2 and 4) and the second letter whether the signal corresponds to uncomplexed (u) or complexed (c) species.

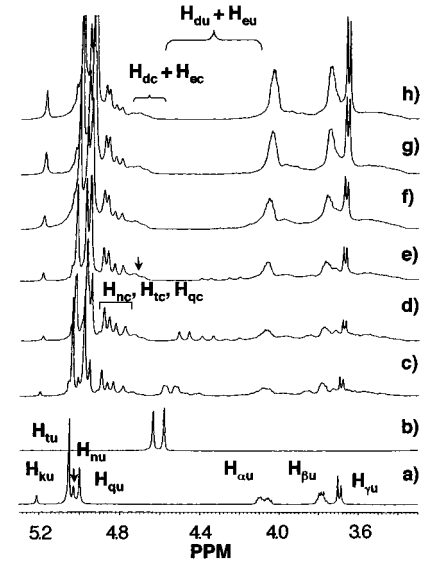

Figure 8. The aliphatic region of ^{1}H NMR spectra (400 MHz, 22 °C) of CD_3COCD_3 solutions of homotritopic guest **1a** and third generation monotopic dendron **5** at (a) 0/10, (b) 10/0, (c) 10/10, (d) 10/20, (e) 10/30, (f) 10/40, (g) 10/50, and (h) 10/60 mM initial concentrations. The first letter and number of the subscript designate the proton (see Schemes 2 and 4) and the second letter whether the signal corresponds to uncomplexed (u) or complexed (c) species.

concentration of crown-functionalized dendron **3**, **4**, or **5** was increased, as observed with the model system **1a**/DB24C8 (Figure 3).

The ethyleneoxy protons of the dendrons are complicated because of the substituted crown ether's intrinsic dissymmetry (Scheme 2). The ethyleneoxy protons of the complexed crown ether moieties of the dendrons are even more complicated due to the enantiotopism (and possibly geometic isomerism) (Scheme 3b) and afford no quantitative information. The signals for the benzylic protons of the dendrons (Scheme 2) undergo distinguishable upfield chemical shifts upon complexation (Figures 7 and 8),[21] which may be explained in terms of the interaction of neighboring complexed dendron units. Because of the additional aromatic protons present in dendrons **3**, **4**, and **5**, most of the aromatic proton signals of the homotritopic core **1a** are not readily analyzed, although importantly H_{au} at 7.96 ppm was clearly resolved and integratable in all cases, as with the model system **1a**/DB24C8.

The second and third generation dendritic systems were quantitatively analyzed via the "uncomplexed" (i.e., time averaged exo hydrogen bonded complexed[25,26] and truly uncomplexed) NCH_2 signals assigned as discussed above for the model system: the downfield pair to **1a**, the next upfield pair to the [2]-pseudorotaxane **7**, and the most upfield pair to the [3]pseudorotaxane **8** (Scheme 4), keeping in mind that the two peak intensities in a pair were equal. Distinct signals could be observed and integrated up to 30 mM dendron (above a certain concentration only the downfield signal of the [3]pseudorotaxane **8** was clearly resolved, and its integral was doubled for the estimation). The diminishing signals all gradually merged with the α-ethyleneoxy multiplet at high dendron concentrations. Integration of the 7.96 ppm peak for H_{au} of **1a** provided corroboration of the concentration of this species. This method could not be used with the first generation system because $H_{du} + H_{eu}$ overlaps with complexed α-ethyleneoxy signals (see Figure 7e−g).

For the first generation system based on **3**, determination of the concentrations of uncomplexed **1a** and pseudorotaxanes **7c** and **8c** was achieved via the signals for H_{au} (7.96 ppm), H_{a2} (7.76 ppm), and H_{a3} (7.73 ppm); the concentrations of **9c** were determined by difference.

Because the concentrations of **1a**, [2]pseudorotaxanes **7**, [3]-pseudorotaxanes **8**, and [4]pseudorotaxanes **9** were known, the association constants were known (Table 3). It is especially noteworthy that the ratios of K_1:K_2:K_3 exceed the statistical ratio expected for independent (noncooperative) binding by the three NH_2^+ sites of **1a**, that is, 3:1:$^1/_3$,[22] demonstrating that *positive cooperativity drives the complexation processes!*

To verify this remarkable result, we constructed Scatchard plots, which are independent of the calculations of the individual association constants (Figure 9). The plots for all three generation dendron systems are clearly nonlinear and possess maxima as expected for positively cooperative binding.[22] By comparison of the overall association constant (K_o) values (Table 3), it is apparent that the extent of cooperativity increases as the size of the dendron increases. We attribute this phenomenon to the dendrons' ability to screen the ionic core (**1a**) from the nonpolar bulk solvent in a micelle-like structure: the larger the dendron, the larger the effect. Evidence in support of the encapsulation of the triammonium ion in the systems derived from the dendrons is afforded by the complexed NH_2^+ signals. In the case of the DB24C8 system in acetone-d_6, the signal is observed as a broad peak at 7.85 ppm (Figure 4) and with first generation system **3** at 7.74 ppm, while in second and third generation systems derived from **4** and **5** it appears as a sharp peak at 8.01 ppm (not shown). This is taken to mean that in the pseudorotaxanes derived from the latter two hosts, exchange of these protons is slow because they are effectively "sealed" in the interior of the assembly. π-Stacking[28a] and T-type N^+C-H- -π interactions[28b] may also play a role.

As shown in Table 1, for noncooperative binding of DB24C8 by **1a**, the K_o value is lower than with second and third

Table 3. Association Constants for Dendritic Psuedorotaxane Complexes, in Acetone-d_6 at 22 °C

host/guest system	$10^{-2} \times K_1$ (M^{-1})	$10^{-2} \times K_2$ (M^{-1})	$10^{-2} \times K_3$ (M^{-1})	$10^{-6} \times K_o$[a] (M^{-1})
3/**1a**	1.6 (±0.5)[b]	0.65 (±0.13)[b]	0.67 (±0.26)[b]	0.70 (±0.64)[d]
4/**1a**	2.5 (±0.6)[c]	1.4 (±0.2)[c]	2.1 (±0.6)[c]	7.4 (±4.8)[d]
5/**1a**	2.4 (±0.4)[e]	2.8 (±0.2)[e]	2.3 (±0.3)[e]	15 (±6)[d]

[a] Overall association constant for formation of [4]pseudorotaxane **9d** or **9e** from 1 mol of **1a** and 3 mol of second or third generation dendron **4** or **5**, respectively; $K_o = K_1K_2K_3$. [b] The molar ratios of **1a**, **7c**, and **8c** were determined by integration of H_{au} (7.96 ppm, 3H, **1a**), H_{a2} (7.76 ppm, 2H, **7c**), and H_{a3} (7.73 ppm, 2H, **8c**); these comprise all of the uncomplexed NCH_2 moieties. The latter two signals ride atop the broad signal for complexed NH_2^+ and were integrated by the cut and weigh method. The total concentration of uncomplexed NCH_2 moieties was determined by integration of $H_{dc} + H_{ec}$ (4.80−4.95 ppm) versus all benzylic OCH_2 signals (4.95−5.30 ppm, 6H: H_q and H_t, Scheme 2). From these parameters, [**1a**], [**7c**], and [**8c**] were determined. From the known concentration of complexed NCH_2 moieties, [**9c**] was calculated by difference. The results from the following initial concentrations of **1a**/**3** were used to evaluate K_1, K_2, and K_3: 10/30, 10/40, 10/50, 10/60 mM/mM. Error bars are the standard deviations. [c] The extent of complexation of the dendron and NCH_2 moieties was determined by (1) integration of H_{nu} (5.26 ppm, 2H) versus all benzylic OCH_2 signals (4.9−5.3 ppm, 14H, H_n, H_q, and H_t, Scheme 2), (2) $H_{dc} + H_{ec}$ (ppm) versus all benzylic OCH_2 signals, (3) $H_{dc} + H_{ec}$ (ppm) versus aromatic protons H_o, H_p, H_r, H_s, H_w, H_y, and H_z (6.4−7.1 ppm, 14H, Scheme 2), and (4) integration of the doublet ($J = 8$ Hz) for H_{wu} (7.00 ppm, 1H) versus aromatic protons H_o, H_p, H_r, H_s, H_w, H_y, and H_z (6.4−7.1 ppm, 14H, Scheme 2). Integration of the pairs of signals for $H_{du} + H_{eu}$ of **1a**, [2]- (**7d**), and [3]-pseudorotaxanes (**8d**) yielded the relative concentrations of these species. The concentration of **1a** was confirmed using the integration of the H_{au} signal at ∼7.96 ppm. The concentration of the [4]pseudorotaxane **9d** was determined by difference. The results from the following initial concentrations of **1a**/**4** were used: for K_1, from 10/10 to 10/30 mM/mM; for K_2 and K_3, from 10/10 to 10/20 mM/mM. Error bars are the standard deviations. [d] Error cited is average deviation from the nominal value calculated using both the maximum and the minimum values for K_1, K_2, and K_3 based on the individual error bars. [e] The extent of complexation was determined by integration of H_{ku} (5.2 ppm, 2H) versus the aromatic protons H_l, H_m, H_o, H_p, H_r, H_s, H_w, H_y, and H_z (6.4−7.0 ppm, 26H, Scheme 2). Integration of the pairs of signals for $H_{du} + H_{eu}$ of **1a**, [2]- (**7e**), and [3]-pseudorotaxanes (**8e**) afforded the relative concentrations of these species. The concentration of **1a** was confirmed by integration of the H_{au} signal at ∼7.96 ppm. The concentration of the [4]pseudorotaxane **9e** was determined by difference. The results from the following initial concentrations of **1a**/**5** were used: for K_1, from 10/10 to 10/20 mM/mM; for K_2 and K_3, from 10/10 to 10/30 mM/mM. Error bars are the standard deviations.

generation dendrons **4** and **5**. K_1 for complexation of the dendrons **3**, **4**, and **5** is less than that with DB24C8. This is taken as a reflection of steric effects with the dendrons that are eventually compensated through cooperative interactions which increase K_2 and K_3 significantly for the dendrons relative to DB24C8. This can be seen by the fact that K_{ave} for **3** (97 M^{-1}) is less than K_a for model ester crown **2b** with monotopic guest **6a**, but K_{ave} for **4** and **5** are equal or greater.

In a solution of homotritopic guest **1a** (10 mM) and third generation dendron **5** (10 mM) at and below −20 °C no uncomplexed dendron could be detected based on the H_{ku} signal (Scheme 2). Thus, at lower temperatures, formation of [4]-pseudorotaxane **9e** is complete. The second generation system **1a**/**4** behaved similarly, yielding only the self-assembled dendrimer **9d**.

B. In $CDCl_3$. Dendrons **3** (Figure 10), **4**,[21] and **5** (Figure 11) as 30 mM solutions were treated with solid homotritopic guest **1a** (in an amount that corresponded to 10 mM if it completely dissolved); equilibrium was reached after ca. 12 h, ca. 2 days, and ca. 3 days, respectively. H_{ec} and H_{dc} appeared at 4.6 and 4.7 ppm in each case, and no uncomplexed NCH_2 signals were observed individually or by careful integration of the 3.4−4.4 ppm region (as was done with **1a**/DB24C8 to detect ∼10% of uncomplexed NCH_2 species).

The signals of H_{a5}, H_{b3c}, and H_{c3c} of [4]pseudorotaxanes **9** (Scheme 4) appear at 7.82, 7.51, and 7.78 ppm, respectively. No signals assignable to uncomplexed aromatic moieties in [2]- or [3]-pseudorotaxanes **7** or **8** were found. Recall that in the model system **1a**/DB24C8, the [3]pseudorotaxane **8a** was observed via H_{b2u} and H_{c2u} (Figure 5). The sharp singlet observed for H_{a5} and well-resolved doublets for H_{bc} and H_{cc} indicate that these signals originate from a single species, confirming the sole existence of the 1:3 complex **9c** and the absence of the [2]- or [3]-pseudorotaxane complexes **7c** and **8c**.

Quantitative evidence of the exclusive formation of [4]-pseudorotaxane dendrimers **9** came from integration of the ^1H NMR spectra. The ratios of integrals of the signals for H_{a5} (Scheme 4) at 7.82−7.84 ppm versus those for $H_{dc} + H_{ec}$ at 4.7 and 4.5 ppm were 0.25, in accord with theory. This was also true before equilibrium was reached, meaning that **1a** dissolves solely as the [4]pseudorotaxanes **9**. In first generation **9c**, the signals for H_{dc}, H_{ec}, H_{qc}, and H_{tc} (Schemes 2 and 4) should integrate in the ratio of 2:2:2:4; indeed, the signals at 4.68, 4.57, 5.12, and 4.99 ppm (Figure 10) integrated in the ratio 2.0:2.0:2.0:4.0, respectively. The stoichiometry of complex from **1a** and third generation dendron **5** was determined to be 1:3 by integration of the signals for H_{dc} and H_{ec} versus complexed benzylic protons H_{kc} (Figure 11, Schemes 2 and 4). The sole existence of the wholly complexed [4]pseudorotaxane dendrimer **9e** was also demonstrated by the integrals of signals for H_{a5}, H_{kc}, and $H_{dc} + H_{ec}$ protons in a 1.0:2.0:4.0 ratio.

Inasmuch as free tritopic guest **1a** and [2]- and [3]-pseudorotaxanes **7** and **8** (Scheme 1) could not be detected in solutions of crown-functionalized dendrons **3**−**5** and **1a** in $CDCl_3$, it was not possible to calculate association constants. However, the percentages of solid **1a** dissolved in 30 mM solutions of the dendrons serve as indicators of the relative K_a values for the three [4]pseudorotaxane complexes **9c**, **9d**, and **9e**. The amount of **1a** in a solution of dendron **3** was determined and corroborated by three methods using the following integrals: (a) H_{a5} (7.84 ppm, 3H) versus the total for H_r, H_s, H_w, H_y, and H_z (6.4−7.0 ppm, 8H), (b) H_{qu} (5.25 ppm, 2H) versus the total for H_{qu}, H_{qc}, H_{tu}, and H_{tc} (4.9−5.4 ppm, 6H) of dendron **3**, and (c) $H_{dc} + H_{ec}$ (4.54 ppm, 12H) versus the total for H_{qu}, H_{qc}, H_{tu}, and H_{tc} (4.9−5.4 ppm, 6H). After equilibration, 58.2 (±2.1)% of **1a** had dissolved, yielding a solution 5.82 (±0.21) mM in total concentration of **1a**, all of it in the form of [4]pseudorotaxane **9c**. The amount of **1a** taken into solution by **4** was determined analogously; the final solution was 5.98 (±0.23) mM in total concentration of **1a**, all in the form of **9d**. A total of 66.6% of **1a** ([**9e**] = 6.66 (±0.30) mM) was taken into the 30 mM solution of third generation dendron **5**; using a 10 mM solution of **5** and an equivalent amount of solid **1a**, the final solution contained 2.25 (±0.12) mM of **9e**. The latter concentration is 20% higher than the monotopic guest **6a** (5.59 mM) in 10 mM **5** (above) on a per NH_2^+ basis. The larger crowned dendrons are more effective hosts than the smaller ones. This is consistent with cooperative binding of **5** by **1a**.

(28) (a) Claissens, C. G.; Stoddart, J. F. *J. Phys. Org. Chem.* **1997**, *10*, 254−272. (b) See: Cantrill, S. J.; Preece, J. A.; Stoddart, J. F.; Wang, Z.-H.; White, A. J. P.; Williams, D. J. *Tetrahedron* **2000**, *56*, 6675−6681 for a discussion of the importance of C−H- - -π bonds in crystals of tetrabenzo-24-crown-8 and leading references to this phenomenon.

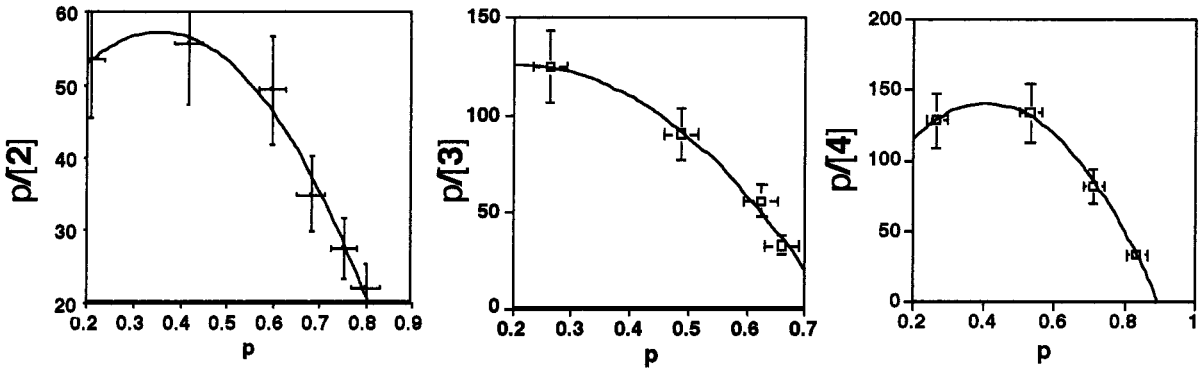

Figure 9. Scatchard plots for complexation of homotritopic guest **1a** with (a) (left) first generation monotopic dendron **3**, (b) (middle) second generation monotopic dendron **4**, and (c) (right) third generation monotopic dendron **5** in CD_3COCD_3 at 22 °C. p = fraction of ammonium sites bound. Error bars in p, ±0.03 absolute; error bars in p/[host], ±15% relative. The lines (second order polynomial fits) are simply to guide the eye.

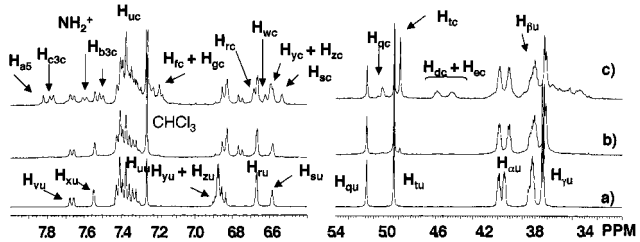

Figure 10. The ^{1}H NMR spectra (400 MHz, 22 °C) of (a) a 30 mM $CDCl_3$ solution of first generation monotopic dendron **3**; a 30 mM $CDCl_3$ solution of **3** mixed with $^1/_3$ mol equiv of solid tritopic guest **1a** after (b) 10 min and (c) 15 h. The first letter and number of the subscript designate the proton (see Schemes 2 and 4) and the second letter whether the signal corresponds to uncomplexed (u) or complexed (c) species.

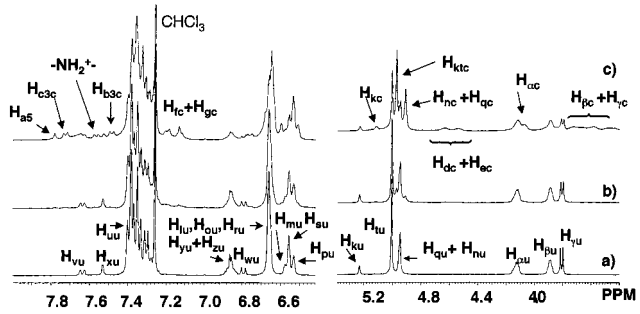

Figure 11. The ^{1}H NMR spectra (400 MHz, $CDCl_3$, 22 °C) of (a) a 30 mM solution of third generation monotopic dendron **5** mixed with $^1/_3$ mol equiv of solid homotritopic guest **1a** recorded (a) immediately, (b) after 10 min, and (c) after 72 h. The first letter and number of the subscript designate the proton (see Schemes 2 and 4) and the second letter whether the signal corresponds to uncomplexed (u) or complexed (c) species.

The slower formation of third generation dendritic [4]-pseudorotaxane **9e** relative to the smaller dendrimers **9c** and **9d** is attributed to steric hindrance experienced by neighboring dendron units. The latter can be deduced from the following two spectroscopic observations. Significant upfield shifts were observed for the complexed benzylic protons of third generation dendron **5**: H_{kc}, H_{nc}, H_{qc}, and H_{tc} in **9e** (Figure 10). In contrast, in the spectra of dendron **5** and monotopic guest **6a** (Figure 7), the signals for these benzylic protons in the [2]pseudorotaxane complex **5**:**6a** were indistinguishable from those of uncomplexed **5**.

Recently, a qualitative observation of cooperativity in the binding of a homotritopic DB24C8 analogue by **1a** in CD_3CN/$CDCl_3$ to form a 1:1 complex containing three pseudorotaxane moieties was reported.[29] This may be termed "entropic cooperativity" since it involves bimolecular complexation of fairly rigid complementary tritopic species. In contrast, the present cooperativity appears to be more enthalpically driven in that it involves four distinct molecules, three of which are very flexible, interacting to form the [4]pseudorotaxanes **9c**−**e**.

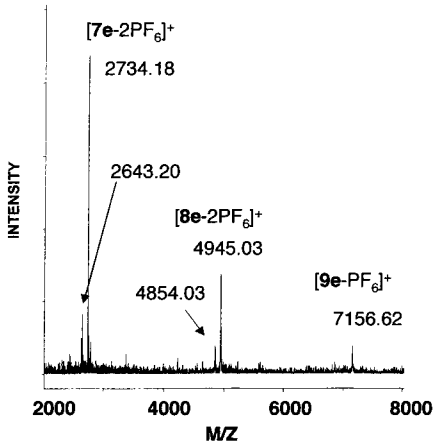

Figure 12. The MALDI-TOF mass spectrum (matrix: DHBA) of a sample prepared by freeze-drying (−78 °C, in vacuo) a solution of homotritopic guest **1a** (2.50 mM) and third generation dendron **5** (7.50 mM) in acetone, showing the presence of third generation dendritic [2]-, [3]-, and [4]-pseudorotaxanes **7e**, **8e**, and **9e** (Scheme 1), respectively.

C. Mass Spectrometry. The dendritic pseudorotaxanes were analyzed by mass spectrometry using samples prepared by freeze-drying acetone solutions of homotritopic guest **1a** with 3 equiv of the dendrons **3**, **4**, and **5**. In each case, the spectrum (either FAB or MALDI-TOF) contains peaks for the self-assembled dendritic [4]pseudorotaxane complex **9**, [3]pseudorotaxane **8**, and [2]pseudorotaxane **7** after losses of PF_6^- counterions.[21] In the case of the second generation system **4**, we note loss of HPO_4^{2-}, a hydrolysis product of PF_6^- as documented in the literature.[30] Figure 12 shows the MALDI-TOF MS for the third generation system **1a**/**5**; peaks at intervals of 91 mass units below $[\mathbf{8e}\text{-}2PF_6]^+$ and $[\mathbf{7e}\text{-}2PF_6]^+$ indicate loss of benzyl groups from the periphery of the dendrons. The

(29) Fyfe, M. C. T.; Lowe, J. N.; Stoddart, J. F.; Williams, D. J. *Org. Lett.* **2000**, *2*, 1221−1224.
(30) Moucheron, C.; Kirsch-De Mesmaeker, A. *J. Am. Chem. Soc.* **1996**, *118*, 12834−12835.

Table 4. Supramolecular Formulas, Calculated Supramolecular Weights, and Observed (MS) Mass/Charge Ratios

structure	molecular formula	calcd MW	obs *m/z*
9c-PF_6	$[C_{48}H_{48}N_3P_2F_{12}(C_{46}H_{50}O_{12})_3]^+$	3339.3	3339.5[a1], 3344.6 [d1]
8c-$2PF_6$	$[C_{48}H_{48}N_3PF_6(C_{46}H_{50}O_{12})_2]^+$	2400.0	2400.2[a2], 2400.8[d2]
7c-$3PF_6$	$[C_{48}H_{48}N_3(C_{46}H_{50}O_{12})]^+$	1460.7	1459.2[a3], 1460.4[d3]
9d-PF_6	$[C_{48}H_{48}N_3P_2F_{12}(C_{74}H_{74}O_{16})_3]^+$	4611.81	4611.06[b1], 4612.5[e1]
8d-$2PF_6$	$[C_{48}H_{48}N_3PF_6(C_{74}H_{74}O_{16})_2]^+$	3248.34	3248.69[b2], 3249.6[e2]
8d-$3PF_6 + Na + 2HPO_4$	$[C_{48}H_{48}N_3(C_{74}H_{74}O_{16})_2(Na)(HPO_4)_2]^+$	3318.38	3318.42[b3]
7d-$2PF_6$	$[C_{48}H_{48}N_3PF_6(C_{74}H_{74}O_{16})]^+$	1884.88	1884.90[b4], 1884.3[e3]
7d-$3PF_6 + Na + 2HPO_4$	$[C_{48}H_{48}N_3(C_{74}H_{74}O_{16})(Na)(HPO_4)_2]^+$	1954.91	1954.93[b5]
9e-PF_6	$[C_{48}H_{48}N_3P_2F_{12}(C_{130}H_{122}O_{24})_3]^+$	7156.81	7156.62[c1]
8e-$2PF_6$	$[C_{48}H_{48}N_3PF_6(C_{130}H_{122}O_{24})_2]^+$	4945.01	4945.03[c2]
8e-$2PF_6$-C_7H_7	$[C_{48}H_{48}N_3PF_6(C_{130}H_{122}O_{24})(C_{123}H_{115}O_{24})]^+$	4853.96	4854.03[c3]
7e-$2PF_6 + H$	$[C_{48}H_{48}N_3PF_6(C_{130}H_{122}O_{24})]^+$	2734.23	2734.18[c4]
7e-$2PF_6 + H$-C_7H_7	$[C_{48}H_{48}N_3PF_6(C_{123}H_{115}O_{24})]^+$	643.18	2643.18[c5]

[a] FAB mass spectrum recorded in the positive ion mode using 3-NBA as the matrix; sample prepared by freeze-drying (−78 °C, in vacuo) an acetone solution 5.00 mM in **1a** and 15.00 mM in **3**. (1) 5%, (2) 6%, (3) taken as base peak. [b] MALDI-TOF mass spectrum recorded in the positive ion mode using *trans*-3-indoleacrylic acid (IAA) matrix; sample prepared by freeze-drying (−78 °C, in vacuo) an acetone solution 2.50 mM in **1a** and 7.50 mM in **4**. (1) 6%, (2) 32%, (3) 15%, (4) taken as base peak, (5) 90%. [c] MALDI-TOF mass spectrum recorded in the positive ion mode using 2,5-dihydroxybenzoic acid (DHBA) as the matrix; sample prepared by freeze-drying (−78 °C, in vacuo) an acetone solution 2.50 mM in **1a** and 7.50 mM in **5**. (1) 9%, (2) 31%, (3) 8%, (4) taken as base peak, (5) 17%. [d] MALDI-TOF mass spectrum recorded in the positive ion mode using DHBA as the matrix; sample prepared as noted above. (1) 4%, (2) 15%, (3) 62% of base peak at $m/z = 666.0$ $[\mathbf{1a} - 2PF_6 - HPF_6]^+$. [e] MALDI-TOF mass spectrum recorded in the positive ion mode using DHBA as the matrix; sample prepared as noted above. (1) 0.7%, (2) 2%, (3) 44% of base peak at $m/z = 559.2$ $[\mathbf{1a} - 2PF_6 - HPF_6 - C_6H_5CH_2NH_2]^+$.

apparent distribution of the complexes indicates partial dissociation/fragmentation of **9e** into subunits **8e** and **7e** during ionization or in the relatively polar matrix. The calculated and observed masses (<0.1% error) of the dendritic pseudorotaxanes are summarized in Table 4.

Conclusions

In acetonitrile and acetone, in which triammonium salt **1a** is soluble, it was possible to detect [2]-, [3]-, and [4]-pseudorotaxane complexes **7a**, **8a**, and **9a** of DB24C8 distinctly by ^{1}H NMR spectroscopy and to estimate association constants. In complexation with DB24C8, the three ammonium sites of **1a** act independently, and hence the three association constants follow the expected statistical ratios. These are believed to be the first association constants measured for [4]-pseudorotaxanes. The nearly exclusive (∼90%) formation of the [4]pseudorotaxane **9a** from the insoluble trisalt **1a** in chloroform is noteworthy. Mass spectrometry was also used to characterize the pseudorotaxanes.

We then demonstrated a concise design and efficient self-assembly of pseudorotaxane dendrimers **9c**−**e**. *In acetone-d_6, complexations of crown functionalized dendrons **3**−**5** with homotritopic guest **1a** are positively cooperative*. Furthermore, the larger dendrons displayed increased association constants. This effect is attributed to encapsulation of the ionic core of the triammonium salt, resulting in screening of the charges from the nonpolar bulk solvent. *In chloroform-d, dendritic [4]-pseudorotaxanes **9c**−**e** are exclusively formed as a result of positively cooperative binding.*

This and related positively cooperative self-assembly approaches offer the possibility of generating larger and more complex supramolecular structures. Encapsulation of guests during the self-assembly process is also an interesting possibility, especially coupled with pH control of this type of reversible pseudorotaxane formation,[31] suggesting several types of applications in addition to those of current interest with covalent dendrimers.[3−9]

Experimental Section

400 MHz ^{1}H NMR spectra were recorded on a Varian Unity with tetramethylsilane (TMS) as an internal standard. Mass spectra were provided by the Nebraska Center for Mass Spectrometry, Lincoln, Nebraska, and also by the Washington University Mass Spectrometry Resource, an NIH Research Resource (grant no. P41RR0954). 1,3,5-Tris[*p*-(benzylammoniomethyl)phenyl]benzene tris(hexafluorophosphate) (**1a**) was prepared according to the literature,[18,20] as was dibenzylammonium hexafluorophosphate (**6a**).[19]

Acknowledgment. The authors gratefully acknowledge financial support by the Chemistry Division of the National Science Foundation through award CHE-9521738 and the Petroleum Research Fund administered by the American Chemical Society (grants 3119-AC7 and 33518-AC7). We are also grateful to Mr. Tom Glass of this Department for his able advice and assistance with regard to the NMR experiments.

Supporting Information Available: Procedures for synthesis of **6b** and **1b**, table of ^{1}H NMR signal assignments for DB24C8/**1a** in CD_3CN, ^{1}H NMR and mass spectra (PDF). This material is available free of charge via the Internet at http://pubs.acs.org.

JA012155S

(31) Ashton, P. R.; Ballardini, R.; Balzani, V.; Gomez-Lopez, M.; Lawrence, S. E.; Martinez-Diaz, M. V.; Montalti, M.; Piersanti, A.; Prodi, L.; Stoddart, J. F.; Williams, D. J. *J. Am. Chem. Soc.* **1997**, *119*, 10641−10651. Ashton, P. R.; Ballardini, R.; Balzani, V.; Baxter, I.; Credi, A.; Fyfe, M. C. T.; Gandolfi, M. T.; Gomez-Lopez, M.; Martinez-Diaz, M.-V.; Morosini, M.; Piersanti, A.; Spencer, N.; Stoddart, J. F.; Venturi, M.; White, A. J. P.; Williams, D. J. *J. Am. Chem. Soc.* **1998**, *120*, 11932−11942. Balzani, V.; Gomez-Lopez, M.; Stoddart, J. F. *Acc. Chem. Res.* **1998**, *31*, 405−414. Ishow, E.; Credi, A.; Balzani, V.; Spadola, F.; Mandolini, L. *Chem.-Eur. J.* **1999**, *5*, 984−989. Balzani, V.; Credi, A.; Venturi, M. In *Stimulating Concepts in Chemistry*; Vögtle, F., Stoddart, J. F., Shibasaki, M., Eds.; Wiley-VCH: New York, 2000; pp 255−266. Balzani, V.; Credi, A.; Raymo, F. M.; Stoddart, J. F. *Angew. Chem., Int. Ed.* **2000**, *39*, 3349−3391. Stoddart, J. F. *Acc. Chem. Res.* **2001**, *34*, 410−411.